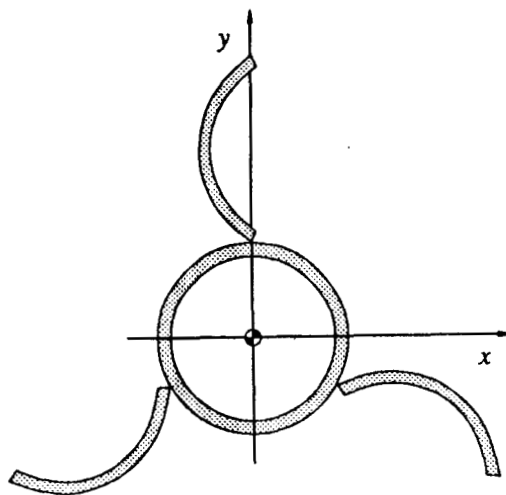


NASA Technical Memorandum 101636

Stability and Dynamic Analysis of a Slender Column with Curved Longitudinal Stiffeners

Mark S. Lake

AUGUST 1989



(NASA-TM-101636) STABILITY AND DYNAMIC
ANALYSIS OF A SLENDER COLUMN WITH CURVED
LONGITUDINAL STIFFENERS (NASA / Langley
Research Center) 67 p

CSCL 20K

N89-27215

Unclas
G3/39 0224569



National Aeronautics and
Space Administration

Langley Research Center
Hampton, Virginia 23665

TABLE OF CONTENTS

	Page
TABLE OF CONTENTS	i
LIST OF TABLES	iii
LIST OF FIGURES	iv
LIST OF SYMBOLS	vi
CHAPTER	
1. INTRODUCTION	1
1.1 Review of Research	2
1.2 Definition of Problem and Objectives	4
2. ANALYSIS	10
2.1 Cross-sectional Geometric Properties	10
2.1.1 Effect of Stiffener Kinematic Attachment on Geometric Properties	11
2.1.2 Calculation of Geometric Properties	14
2.1.3 Optimization Considerations for a Stiffened Column	17
2.2 Analysis of Stiffener Local Buckling	19
2.2.1 Functional Dependence of Stiffener Local Buckling on Geometric Design Parameters ...	20
2.2.2 Derivation of Approximate Explicit Relationship for Stiffener Local Buckling.	24
2.3 Column Design Algorithm	29
3. EXAMPLES AND DISCUSSION	33

3.1	Generation of Design Curves for Example Problems. .	33
3.2	Discussion of Results	39
4.	CONCLUSIONS	44
	REFERENCES	47
	APPENDIX A	
	Derivation of Stiffener Cross-Sectional Inertias	49
	APPENDIX B	
	<u>D</u> esign of <u>S</u> tiffened <u>C</u> olumn <u>C</u> ode (DESTCO)	51
	APPENDIX C	
	Vibration Frequencies of the Stiffened Column	57

LIST OF TABLES

<u>Table Number</u>	<u>Title</u>	<u>Page Number</u>
2.1	Matrix of Normalized Stiffener Local Buckling Stresses From VIPASA Analysis	26
3.1	Nominal Dimensions for Example Central Columns	34
3.2	Design Data for Space Station Freedom Column.	34
3.3	Design Data for Precision Segmented Reflector Column.	34

LIST OF FIGURES

<u>Figure Number</u>	<u>Title</u>	<u>Page Number</u>
1.1	Section of a cylindrical column with curved deployable stiffeners	2
2.1	Symmetry of stiffened column cross section.	14
2.2	Stiffened column cross-sectional geometric parameters	15
2.3	Stiffener local buckling mode due to uniform axial compression.	20
2.4	Typical plot of curved stiffener as represented in VIPASA	25
2.5	Plot of normalized stiffener local buckling stresses from VIPASA analysis.	26
2.6	Comparison of normalized stresses from VIPASA and explicit expression.	28
3.1	Stiffener thickness variation with arc angle for minimum mass designs . .	35
3.2	Minimum mass design curve for Space Station Freedom column	36
3.3	Minimum mass design curve for Precision Segmented Reflector column. .	36
3.4	Verification of Space Station Freedom column design curve	38
3.5	Design curve for Space Station Freedom column including 10% mechanism mass.	39
3.6	Comparison of approximate and exact design curves for Space Station Freedom column including 10% mechanism mass	41
3.7	Family of approximate general stiffened column design curves	42
A.1	Cross-sectional parameters for stiffener moments of inertia	50
B.1	Flow chart of DESTCO program	51
C.1	General Stiffened column design curves with vibration frequency increase .	59

LIST OF SYMBOLS

A	cross-sectional area
a_1, a_2, a_3	coefficient expressions defined for use in equations for moment of inertia
b_1, b_2, b_3, b_4	constants used in bilinear equation for stiffener local buckling stress
a	distance between discrete stiffener attachment locations
b	width of flat plate
c	constant in column vibration frequency equation
ΔM	percent increase in stiffened column mass from that of the central column
ΔP_{cr}	percent increase in stiffened column buckling load from that of the central column
E	Young's modulus
i	summation index
I_x, I_y, I_{xy}	general cross-sectional moments of inertia
$I, I_{xe}, I_{ye}, I_{xye}$	equivalent cross-sectional moments of inertia of stiffened column
I_{cc}, I_{sx}, I_{sy}	cross-sectional moments of inertia of central column and stiffener
l	column length
M_m	stiffener deployment mechanism mass as a percentage of the mass of the central column
μ	mass density
N	number of data points used in least-squares approximation of stress function
ν	Poisson's ratio

P_{cr}	critical buckling load of column
ψ	arc angle of stiffener
ϕ	deployment angle of stiffener
Φ	deployment angle of stiffener which maximizes cross-sectional moment of inertia
r	radius of curved shell
ρ	radius of gyration of cross section
r_i, r_o, r_p	inner and outer radii of central column, and outer radius of stiffener
r_s	average radius of stiffener
σ_s	local buckling stress of stiffener
σ_e	Euler buckling stress
t	thickness of curved shell
t_{cc}	thickness of central column
t_s	thickness of stiffener
θ	orientation angle of moment of inertia reference axis
α, β	surrogate angles defined for use in equations for moment of inertia
ω	vibration frequency of stiffened column
ω_o	vibration frequency of column without stiffeners

CHAPTER 1

INTRODUCTION

A significant percentage of future manned and unmanned space flight missions will involve very large spacecraft whose components will be of such size and/or number as to require on-orbit assembly and integration. Although the goals of these missions may be quite different, the design of these spacecraft gives rise to at least one significant common technological requirement. This requirement is to develop the ability to construct and operate large, lightweight structures in space.

Most of these structures share the characteristic that their design is primarily driven by stiffness as opposed to strength considerations. This along with the constraint of low packaged volume allowances tends to drive the use of very long slender truss members. However, many of these structures are also required to withstand significant loads due to thermal gradients, spacecraft operations, and attitude control maneuvers. Consequently, stability of these slender members becomes a design concern. As a compromise, concepts have been developed for truss members which exhibit high buckling loads and, yet, package very efficiently.

One of these concepts consists of a cylindrical central column having three deployable longitudinal stiffeners each of which are sections of a right circular cylinder with an inner diameter equal to the outer diameter of the central column as shown in Fig. 1.1. While packaged, the stiffeners lie flush around the outside of the central column, and when deployed, the stiffeners are rotated outward to an angle which maximizes the moment of inertia of the cross section. This thesis is the summary of a study of the deployable curved stiffener concept. Results presented herein demonstrate the stability characteristics of columns employing these stiffeners, and outline a procedure for designing these columns for application to large space structures.

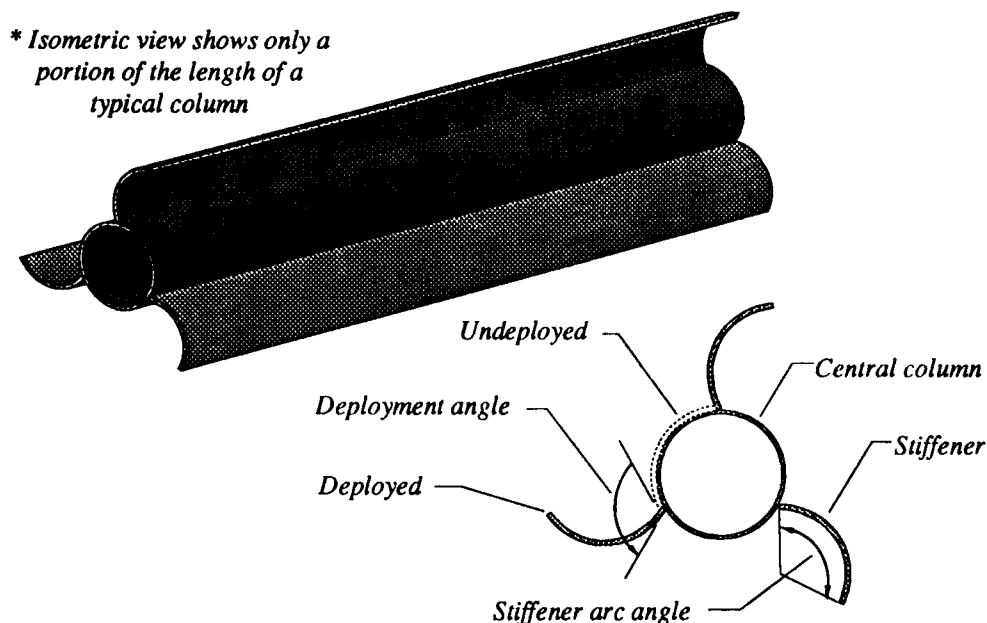


Figure 1.1. Section of a cylindrical column with curved deployable stiffeners.

1.1 Review of Research

Technology development programs have been in existence for more than ten years to address the problem of constructing and operating large, lightweight structures in space. From these programs, concepts have been developed for large truss systems to support a variety of large aperture antennas and platforms (1, 2) and a permanently manned Space Station (3). Typically, these truss systems share the design goals of high stiffness, low weight, and low packaged volume (4, 5). Constrained optimization studies have been conducted to determine geometric proportions of minimum mass structures using constant diameter cylindrical columns (6, 7, 8). Results from these studies support the use of truss members having the maximum diameters allowed for packaging, and lengths which are set by local buckling or vibration requirements.

The issue of improving member buckling loads without reducing member lengths has given rise to a number of design concepts for columns which retain efficient packaged volumes. References 8 and 9 describe a nestable tapered column concept which allows effectively large diameter columns to be assembled from very compactly packaged tapered

column halves. Results of buckling tests and analyses of nestable tapered columns are presented in reference 10 and verify that greatly improved buckling loads can be achieved for columns of a given length without sacrificing the component packaging efficiency.

Other studies have addressed the use of built-up columns for applications requiring very long spans (4, 11). These columns are assembled from efficiently packaged smaller components using a wide variety of assembly geometries, and they exhibit large buckling loads in proportion to their mass and packaged volume.

The disadvantage to the use of built-up or nestable tapered columns is the requirement for on-orbit component assembly. The increase in truss construction time required because of component assembly will probably be acceptable for missions involving manual assembly of smaller truss structures or automated assembly of larger structures. However, there is certainly a class of missions whose assembly requirements will preclude the use of structural components which must be assembled on-orbit. These missions include large manually assembled structures and any deployable structures. For these missions it might be practical to investigate the use of slender, constant diameter columns with deployable stiffeners.

This column concept was introduced in reference 12, and has the characteristics of achieving a substantial increase in column buckling load for a moderate increase in mass and no change in the packaged dimensions (outer diameter and length) of the column. The utility of the concept is very broad in that it may be substituted with essentially any column in any large space truss structure without affecting the packaging of the structure. The disadvantages are the added complexity and cost of implementing deployable stiffener mechanisms. Furthermore, the geometry of the structure indicates that it will exhibit stability modes in addition to simple Euler column buckling that must be accounted for during design.

The study presented in reference 12 considered only column geometries which behaved as simple Euler columns. The objectives of that study were to evaluate stiffener attachment schemes and determine the finite element modeling complexity necessary to predict Euler buckling behavior in the column. The results showed that certain stiffener

attachment schemes greatly improved column buckling load whereas others showed less of an improvement. Also, it was determined that modeling this type of structure with flat plate finite elements requires the use of a very fine mesh to ensure solution accuracy.

The present study focuses on the analysis of stiffener local buckling and derivation of an explicit empirical expression to determine this behavior. This expression is incorporated into a column design routine which determines minimum mass geometric proportions of the stiffeners such that Euler buckling remains the fundamental stability mode of the column. Classical work by Donnell (13) and Timoshenko (14) resulted in explicit expressions for local buckling of long slender curved panels for a variety of loadings and boundary conditions. However, it will be demonstrated that none of these solutions are applicable to the present problem.

1.2 Definition of Problem and Objectives

The stiffened column concept requires hinge mechanisms to attach the stiffeners to the central column. These mechanisms are perceived to be more complex than basic hinges because they must allow free rotation of the stiffener during deployment and yet firmly lock the stiffener in its deployed position to provide maximum resistance to stiffener local buckling. Furthermore, the efficient analysis of large space structures constructed from many of these columns requires the normal operating axial stiffness of the columns to be linear. This requirement may be satisfied in one of two ways. First, it may be possible to design a stiffener hinge mechanism which not only freezes rotational motion upon deployment, but also freezes axial motion, and thus provides an ideal (zero free play) shear load transfer between the central column and the stiffener. Or, second, it may be desirable to isolate the stiffeners from the central column by mounting the hinges to cylindrical collars which slip over the outside of the central column. This approach allows a transfer of only lateral load and no shear load between the central column and the stiffeners and thus removes the stiffeners from the normal operating load path which is primarily axial tension or compression of the central column.

The study presented in reference 12 identified three stiffener kinematic attachment schemes which represent the behavior of possible stiffener hinge designs. The first

kinematic attachment scheme allows the stiffeners to move independently of the central column and each other in the axial direction while all move together in the lateral direction. This scheme represents a design which uses hinges with no shear load transfer capability but rigid restraint against stiffener rotation. The second kinematic attachment scheme allows shear load transfer between individual stiffeners but not between the stiffeners and the central column while all components move together in the lateral direction. This scheme represents a design which uses hinges that become rigid in both rotation and shear upon deployment, but the stiffeners and hinges are attached to isolation collars which slide along the central column. The third kinematic attachment scheme allows direct shear and rotational load transfer between the stiffeners and the central column. This scheme represents a design which also uses hinges that become rigid in both rotation and shear upon deployment, but in this case the hinges are attached directly to the central column.

All three kinematic attachment schemes result in column designs which exhibit linear axial stiffness within the normal operating tension and compression load range. For the first two attachment schemes this axial stiffness is simply the axial stiffness of the central column, and for the third it is the stiffness of the central column plus that of the stiffeners. The difference in these kinematic attachments is the way in which they allow the stiffeners to influence the stability of the central column. It will be shown that stiffened columns may exhibit either linear or nonlinear stability behavior. The nature of the fundamental or lowest stability mode will depend upon the type of kinematic attachment used for the stiffener and the geometric proportions of the stiffener and central column.

$$P_{cr} = \frac{\pi^2 EI}{l^2} \quad (1.1)$$

It is apparent that any of these kinematic attachments would result in columns having one stability mode which could be predicted using simple linear Euler theory for a simply supported column (Eq. 1.1). This should be obvious for a column using the third kinematic attachment scheme because it would be a simple prismatic column directly obeying the assumptions of Euler theory. The first and second kinematic attachment schemes can also be understood to give rise to simple linear Euler behavior if one realizes the stiffener contributions in these cases can be viewed as distributed lateral elastic restraints. Results were presented in reference 12 which verified Euler column behavior

for test specimens constructed with each of the three kinematic attachment schemes described. It should be noted that the effective cross-sectional moment of inertia, I , in Eq. 1.1 depends on the stiffener kinematic attachment scheme employed.

In addition to the simple linear Euler stability modes described, a column designed with rigidly fixed stiffeners (third kinematic attachment scheme) would also have linear stiffener local buckling modes. These modes are similar to those predicted for stiffened panels under uniform axial compression (15), and they would be characterized by lateral flexing of the stiffeners with sinusoidal amplitude variation along the column length and essentially no lateral motion of the central column. A number of classical linear solution procedures exist for calculating the local buckling stress of stiffeners with simple cross-sections. Furthermore, many linear numerical procedures exist for calculating the local buckling stress of stiffeners with complex cross-sections. Therefore, it is a relatively straightforward task to analyze the critical loads of stiffened columns exhibiting linear stability behavior.

Brush and Almroth (16) have outlined general situations in which nonlinear analysis is needed to capture stability behavior. One of these situations is represented by stiffened columns employing either the first or second stiffener kinematic attachment scheme. These kinematic attachments allow only lateral load to be transferred between the stiffeners and the central column. Since the central column is nominally straight and loaded through uniform axial compression, the only way for the stiffeners to become loaded is through a lateral motion of the central column. This lateral motion can be determined with linear analysis and is equivalent to Euler column buckling. However, since this lateral motion only occurs as a result of passing a linear bifurcation point, predicting local stiffener instability beyond this point using common numerical routines such as finite element analysis may require nonlinear solution procedures.

The present study will only address linear stability analyses of the stiffened column. These analyses will include Euler column buckling and linear local buckling of a uniformly compressed stiffener. Therefore, the results are most applicable to columns designed with hinge mechanisms which become rigid upon deployment (the third stiffener kinematic attachment scheme).

The primary stability design goal of this type of stiffened column is simply to ensure that its fundamental buckling mode is an Euler column mode, and thus, the value of the corresponding buckling load can be predicted using Eq. 1.1. Providing this guarantee requires the ability to analyze the possible stiffener local buckling modes and relate the corresponding critical loads to the design parameters of the column.

As stated previously, the problem of stiffener local buckling is represented by a slender curved panel under uniform axial compression. Donnell (13) and Timoshenko (14) have generated solutions for the stability of curved panels under uniform compression for a variety of boundary conditions, and in some cases have been successful in deriving exact explicit expressions for the critical stress. The boundary conditions applicable to this problem are a clamped connection along one of the stiffener's generators, free along the other, and pinned at both ends. The exact solution for this combination of boundary conditions and applied loading has not been generated to date, however, because of the character of the governing differential equations it can be shown that this solution would have the form of a transcendental eighth-order system of equations. A solution of this form would offer little insight to the relationship between the critical stress and the geometric parameters of the column.

Since no exact explicit expression exists to characterize this behavior, a reasonable alternative is to generate an approximate explicit expression based on empirical results. These results may be generated in a number of ways. First, it is certainly possible to construct a family of test specimens which represent the expected range of design parameters, and base the empirical expression on experimental data accumulated from these specimens. Second, it is possible to derive the transcendental eighth-order system of equations representing the exact solution to the governing differential equations, and generate a family of analytical data from iterative numerical solution of this system. Third, it is possible to employ existing numerical structural analysis techniques (e.g. finite element method or the finite strip method) to generate numerical results.

The obvious disadvantage in obtaining results through experimental study is the cost and time necessary to construct and test an adequate series of specimens. Therefore, numerical analysis techniques may be better suited for this task. Such techniques have been demonstrated to be very accurate for linear stability calculations. Probably the most

widely used numerical structural analysis technique is the finite element method. Results presented in reference 12 indicate that applying this technique to the modeling of a slender stiffened column would require a very fine mesh and result in excessive solution times to ensure solution accuracy. This is very undesirable for an analytical study requiring the generation of a set of parametric solutions.

Alternatively, references 17 and 18 describe an efficient and accurate solution technique using a linked-plate representation of the structure. This technique is used to model prismatic branched plate or shell structures acted upon by longitudinally invariant loads as assemblies of thin flat plate strips rigidly connected along their longitudinal edges. The two-dimensional plate equations describing each plate strip are reduced to one-dimensional equations through the assumption of sinusoidal longitudinal deformations, and a generalized stiffness matrix representing the structure is assembled from equilibrium and compatibility considerations. Reference 18 describes the structural analysis code VIPASA which generates this linked-plate representation of the structure and uses it in the solution of linear stability and vibration problems.

There are two fundamental advantages to using the VIPASA routine for analysis of prismatic branched plate and shell structures with longitudinally invariant applied loadings. First, the solution accuracy is guaranteed for structures which obey the kinematic constraints imposed. This is because it is a numerical solution to the linear differential equations governing the structure. Second, by reducing the 2-D plate theory to a 1-D theory, the size of the problem is greatly reduced and, consequently, the solution times are very small compared to other routines such as those based on finite element analysis. Because of these considerations, all stability calculations for the present study are performed using the VIPASA analysis routine imbedded in the design optimization code, PASCO (19, 20).

The present study focuses on the derivation of an approximate empirical expression for buckling of a curved stiffener, clamped along one edge and free along the other. The solution is sought for bounded ranges of the stiffener geometric parameters. The bounds for these ranges are derived from considerations set forth by typical large space structure design studies. The empirical expression for stiffener local buckling is used in formulating design rules for stiffened columns which exhibit Euler buckling as a fundamental stability

mode. Additionally, studies are conducted on the cross-sectional moment of inertia of the stiffened column to develop rules governing mass minimization of the design. Finally, these results are assembled in a computer design program which is used to generate stiffened column designs for two current large space structure applications.

CHAPTER 2

ANALYSIS

This chapter is a summary of analyses performed to derive rules governing the minimum mass design of a slender cylindrical column stiffened with curved deployable stiffeners. These rules are determined from two sources: 1) consideration of equivalent cross-sectional properties, and 2) consideration of stiffener stability. The first section of the chapter deals with calculation of equivalent cross-sectional properties. These properties determine column mass, packaged size, and equivalent flexural stiffness, and a knowledge of their functional dependence on the cross-sectional geometric parameters leads to minimum mass design rules. The second section of the chapter outlines analyses performed to determine an approximate explicit expression governing stiffener local buckling. This expression is used to define a design condition that guarantees Euler buckling as the fundamental stability mode of the column. The third section of the chapter outlines the development and use of a stiffened column design procedure. Finally, a computer program which automates the design procedure is discussed as well as the steps for employing it in a design exercise.

2.1 Cross-sectional Geometric Properties

As previously stated, the ultimate goal in the design of a stiffened column is insuring the fundamental stability mode of that column to be Euler buckling. Given that consequence, the column can be characterized by equivalent properties such as the cross-sectional area and moment of inertia. Calculating these properties involves evaluating double integrals over the column cross section. Derivations for these equivalent properties will be presented later. First, the general nature of the cross section will be examined in detail in order to simplify the equivalent representation of the column.

2.1.1 Effect of Stiffener Kinematic Attachment on Geometric Properties

As stated in the introduction, the equivalent cross-sectional properties of the stiffened column depend not only on the cross-sectional shape but also on the stiffener kinematic attachment scheme. Stiffened columns employing any of the three attachment schemes identified in the introduction can be represented by one of two distinct equivalent members. One of these equivalent members represents the first stiffener attachment scheme (no shear load transfer between stiffeners or the stiffeners and the central column). The other equivalent member represents either the second or the third stiffener attachment scheme (ideal shear load transfer between stiffeners, and either ideal or no shear load transfer between the stiffeners and the central column).

A stiffened column using either the second or third stiffener attachment scheme is represented by a single member having the equivalent moment of inertia of the entire cross section about axes centered at its centroid. This is seen clearly for the third attachment scheme in which the stiffeners are rigidly attached and represent simple extensions of the central column. This also applies to the second attachment scheme in which the stiffener assembly behaves as one member and the central column behaves as another so that the equivalent moment of inertia is the sum of the inertias of the two components with respect to their respective centroids. However, due to symmetry, the two components have the same centroid location. Thus, summing their moments of inertia with respect to their respective centroids is equivalent to calculating the moment of inertia of the entire section.

A stiffened column using the first stiffener attachment scheme can be thought of as an assembly of members which assume the same lateral deflection without any shear load transfer between them. The equivalent cross-sectional moment of inertia of this assembly is simply the sum of the inertias of the individual elements with respect to their respective centroids, and consequently, the flexural stiffness of the column is the Young's modulus times this equivalent moment of inertia. Before concentrating on stiffened columns employing the third stiffener attachment scheme, a short discussion is presented to explain the consequences of employing the first stiffener attachment scheme.

The flexural stiffness of a column employing the first kinematic stiffener attachment

scheme has some interesting characteristics which can be determined by employing the procedure just established for calculating its equivalent cross-sectional moment of inertia. The total moment of inertia is simply the sum of the inertias of the individual components about their respective centroids. Expressions for the moments of inertia of two of the stiffeners can be derived from the the moments of inertia of the remaining stiffener by applying axis rotation transformations known to be as follows (21):

$$\begin{aligned} I_x' &= I_x \cos^2 \theta + I_y \sin^2 \theta - I_{xy} \sin 2\theta \\ I_y' &= I_y \cos^2 \theta + I_x \sin^2 \theta + I_{xy} \sin 2\theta \\ I_{xy}' &= \frac{I}{2} (I_x - I_y) \sin 2\theta + I_{xy} \cos 2\theta \end{aligned} \quad (2.1)$$

where I_x , I_y , and I_{xy} are the cross-sectional moments of inertia in the original coordinate system, θ is the angle of rotation of the coordinate system, and I_x' , I_y' , and I_{xy}' are the cross-sectional moments of inertia in the rotated coordinate system.

It should be noted that, relative to a given stiffener, one of the others is rotated by $2\pi/3$ and the remaining one is rotated by $-2\pi/3$. Therefore, applying the transformation and summing the resulting inertias gives:

$$\begin{aligned} I_{xe} &= I_{cc} + \frac{3}{2} (I_{sx} + I_{sy}) \\ I_{ye} &= I_{cc} + \frac{3}{2} (I_{sx} + I_{sy}) \\ I_{xye} &= 0 \end{aligned} \quad (2.2)$$

where I_{xe} , I_{ye} , and I_{xye} are the equivalent cross-sectional moments of inertia, I_{cc} is the moment of inertia of the central column relative to its centroid, and I_{sx} and I_{sy} are the principal moments of inertia of one of the stiffeners relative to its centroid.

Two very interesting results are shown in Eq. 2.2. First the equivalent product of inertia, I_{xye} , of the cross section is equal to zero despite the fact that the individual stiffeners may have a non-zero product of inertia. Second, the equivalent moments of inertia about the x and y axes are identical. These two results taken together dictate that the equivalent moment of inertia of the cross section has only one value, independent of the orientation angle of the reference axis. This is certainly significant and desirable from the standpoint that it precludes the column from having a preferred direction of Euler buckling.

Another significant characteristic is that the same expression will result (Eq. 2.2) regardless of the value of stiffener deployment angle (see Fig. 1.1). This can be understood by realizing two points. First, the constraint that the stiffeners differ in orientation by $2\pi/3$ exists independently of deployment angle. Second, the reference axes can always be oriented parallel to the principal axes of one of the stiffeners so I_{sx} and I_{sy} will have the same value for any deployment angle. Therefore, not only is the equivalent cross-sectional moment of inertia for a given deployment angle independent of the orientation angle of the reference axis, but the value of the moment of inertia is also independent of deployment angle. Thus, the cross section has the same equivalent flexural stiffness regardless of whether or not the stiffeners are deployed.

These results contribute valuable information for the design of a stiffened column. It is obvious that designing a column with hinges having no shear load transfer capability would be pointless. The same improvement in equivalent cross-sectional moment of inertia could be achieved with less added mass by simply increasing the thickness of the central column. Thus, only the columns with stiffeners attached through hinges having effectively rigid shear load transfer capability are further analyzed. These correspond to the second and third kinematic attachment schemes.

The independence of cross-sectional moment of inertia with reference axis orientation can also be demonstrated for columns employing stiffener hinges with rigid shear load transfer capability. A rigorous mathematical proof of this point would involve rather lengthy expressions and, therefore, an equally conclusive proof by deduction is performed. The basis of this proof is the fact that the moment of inertia of a cross section made up of three infinitesimal area elements located at the vertices of an equilateral triangle is independent of the orientation of the reference axis.

Each stiffener in the stiffened column cross section can be broken up into a large number of differential area elements with each element having corresponding elements on both of the other stiffeners as indicated in Fig. 2.1. Due to symmetry, at any arbitrary deployment angle, these three differential elements are all located the same radial distance from the centroid of the cross section and the same distance from each other. Therefore, the three differential area elements are located at the vertices of an equilateral triangle whose centroid is coincident with the centroid of the cross section. Consequently, the moment of inertia of these three area elements is independent of the reference axis orientation for any arbitrary deployment angle. Furthermore, the moment of inertia of the stiffener assembly is simply the sum of the inertias of a set of differential triangles subdividing the stiffener assembly cross section, and therefore this moment of inertia is also independent of the reference axis orientation. Finally, the total moment of inertia of the cross section is the sum of the inertia of the stiffener assembly and that of the central column, and thus, this quantity is also independent of reference axis orientation angle.

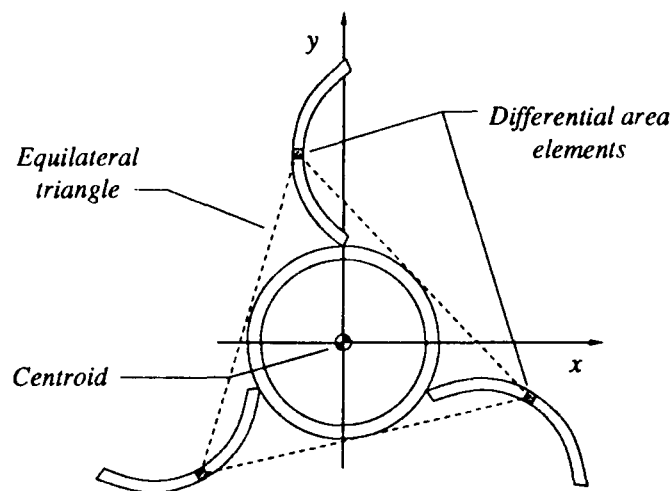


Figure 2.1. Symmetry of stiffened column cross section.

2.1.2 Calculation of Geometric Properties

The previous result establishes that it is only necessary to calculate one equivalent cross-sectional moment of inertia to completely characterize the flexural stiffness of the

stiffened column. The following derivation of this expression is performed assuming arbitrary values for all cross-sectional geometric parameters. Referring to Fig. 2.2, these parameters include central column inner radius (r_i) and outer radius (r_o), stiffener outer radius (r_p), arc angle (ψ), and deployment angle (ϕ).

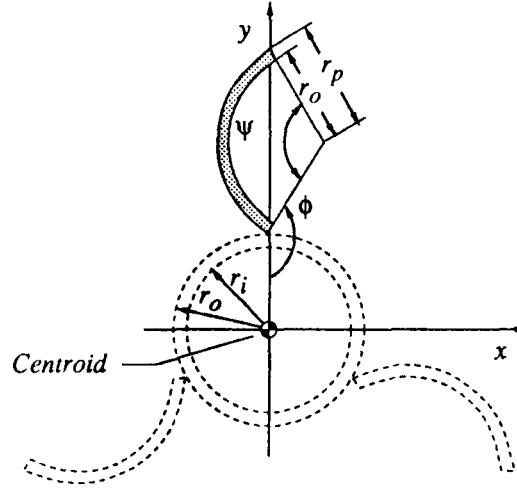


Figure 2.2. Stiffened column cross-sectional geometric parameters.

It should be apparent that Eq. 2.2, which were derived for a column using stiffener attachment hinges with no shear load transfer capability, are also applicable to the derivation of the equivalent cross-sectional moment of inertia for columns using hinges with a rigid shear connection. The only modification necessary is that for the later case, I_{xx} and I_{yy} denote the x and y moments of inertia of the stiffener relative to the centroidal coordinate axes of the entire cross section. Given these definitions, it is possible to derive the following expressions for these component moments of inertia. The derivation of these expressions is given in Appendix A.

$$\begin{aligned}
 I_{xx} = & a_1 (1 - \cos\phi)^2 - a_2 (1 - \cos\phi) \left(\cos\alpha - \cos(\alpha - \psi) \right) \\
 & + a_3 \left\{ \psi/2 - \left(\sin 2\alpha - \sin 2(\alpha - \psi) \right) / 4 \right\} \\
 I_{yy} = & a_1 \sin^2\phi + a_2 \sin\phi \left(\sin\alpha - \sin(\alpha - \psi) \right) \\
 & + a_3 \left\{ \psi/2 + \left(\sin 2\alpha - \sin 2(\alpha - \psi) \right) / 4 \right\}
 \end{aligned} \tag{2.3}$$

where:

$$\begin{aligned}
 a_1 &= \frac{\psi}{8} (r_p^2 - r_o^2) (r_p + r_o)^2 \\
 a_2 &= \frac{1}{3} (r_p^3 - r_o^3) (r_p + r_o) \\
 a_3 &= \frac{1}{4} (r_p^4 - r_o^4) \\
 \alpha &= \frac{\pi}{2} + \phi + 2 \tan^{-1} \left(\frac{r_p - r_o}{2(r_p + r_o)} \right)
 \end{aligned} \tag{2.4}$$

Additionally, the moment of inertia of the central column is derived in reference 21, and the expression follows.

$$I_{cc} = \frac{\pi}{4} (r_o^4 - r_i^4) \tag{2.5}$$

Substituting Eq. 2.3 and 2.5 into Eq. 2.2 gives the expression for the cross-sectional moment of inertia of a stiffened column. After simplification using trigonometric identities, this expression becomes:

$$\begin{aligned}
 I &= \frac{\pi}{4} (r_o^4 - r_i^4) + 3a_1 (1 - \cos \phi) \\
 &+ 6a_2 \sin \left(\frac{\psi}{2} \right) \sin \left(\frac{\phi}{2} \right) \cos \left(\frac{(\phi + \psi - 2\alpha)}{2} \right) + \frac{3a_3 \psi}{2}
 \end{aligned} \tag{2.6}$$

A similar procedure may be followed to obtain the expression for cross-sectional area of the stiffened column. This derivation is very straightforward and the result is given in Eq. 2.7 without presentation of the details.

$$A = \frac{3\psi}{2} r_p^2 + \left(\pi - \frac{3\psi}{2} \right) r_o^2 - \pi r_i^2 \tag{2.7}$$

2.1.3 Optimization Considerations for a Stiffened Column

As mentioned in the introduction, the primary design goal of the stiffened column is to produce columns whose fundamental stability mode is Euler buckling, and, consequently, whose buckling load will be proportional to the cross-sectional moment of inertia presented in Eq. 2.6. Therefore, mass optimization of a column having a certain length involves simply minimizing the cross-sectional area of the column for a given cross-sectional moment of inertia. It is reasonable to assert that minimizing the cross-sectional area for a given moment of inertia is equivalent to the conjugate task of maximizing the moment of inertia for a given area. Performing this conjugate optimization will prove more useful for many applications; because a common set of design constraints is a maximum mass allowance and maximum packaged size allowance (outer radius of stiffeners, r_p).

The first issue to be addressed in obtaining the maximum moment of inertia for a given area is calculation of the optimum stiffener deployment angle. Eq. 2.7 demonstrates a straightforward observation that the cross-sectional area is not dependent on the stiffener deployment angle. Furthermore the trigonometric functions in Eq. 2.6 having ϕ as an argument can only go through at most one half cycle for the whole range of allowed values of ϕ , ($0 \leq \phi \leq \pi$). Therefore, there exists a unique value for the deployment angle which will produce a maximum cross-sectional moment of inertia for given values of the other cross-sectional geometry parameters (r_i , r_o , r_p , and ψ). This value can be determined by differentiating Eq. 2.6 with respect to ϕ , setting the resulting expression equal to zero, and solving for ϕ . Differentiating Eq. 2.6 with respect to ϕ gives:

$$\frac{\delta I}{\delta \phi} = 3a_1 \sin \phi + 6a_2 \sin \left(\frac{\psi}{2} \right) \left[\frac{1}{2} \cos \left(\frac{\phi}{2} \right) \cos \left(\frac{(\phi + \psi - 2\alpha)}{2} \right) + \frac{1}{2} \sin \left(\frac{\phi}{2} \right) \sin \left(\frac{(\phi + \psi - 2\alpha)}{2} \right) \right]$$

Reducing this expression using trigonometric identities and the definitions in Eq. 2.4, and equating it to zero, gives the following:

$$0 = a_1 \sin \phi + a_2 \sin \left(\frac{\psi}{2} \right) \cos \left(\alpha - \frac{\psi}{2} \right)$$

Since the surrogate angle α is defined in terms of ϕ (see Eq. 2.4), it is necessary to further employ trigonometric identities to solve the above expression for ϕ . After this is done the following expression is derived for the deployment angle, Φ , which maximizes the cross-sectional moment of inertia for given values of the stiffener radii and arc angle.

$$\Phi = \tan^{-1} \left(\frac{a_2 \sin(\psi/2) \cos(\beta)}{a_2 \sin(\psi/2) \sin(\beta) - a_1} \right), \quad 0 \leq \Phi \leq \pi \quad (2.8)$$

where:

$$\beta = \frac{\pi}{2} - \frac{\psi}{2} + 2 \tan^{-1} \left(\frac{r_p - r_o}{2(r_p + r_o)} \right) \quad (2.9)$$

Eq. 2.6, 2.7, and 2.8 represent three constraint conditions on the design of a stiffened column. The next section will address stiffener stability analyses which will lead to one more design condition. That will bring the total number of conditions to four, with the total number of unknown parameters equal to seven (r_i , r_o , r_p , ϕ , ψ , I , and A). Obviously, most truss applications will also specify the column buckling load and, thus, through Eq. 1.1, specify the moment of inertia, I . With this additional constraint, the total number of conditions come to five for the seven specified parameters.

Although the system is still indeterminate at this point, it would certainly be possible to locate a minimum column mass. However, performing this optimization will invariably produce a design in which $r_p \rightarrow \infty$, causing the cross-sectional area and, consequently, the mass to become infinitesimal. The implication of this is simple; without imposing constraints on the magnitudes of the column radii, mass optimization produces no useful results. Furthermore, this argument can be extended to show that the only way of producing useful designs from a mass optimization routine is to make the routine determinate by supplying two independent constraints on the column radii.

The example of mass minimization with no constraints on column radii was just

shown to result in designs in which $r_p \rightarrow \infty$. Similarly, applying only one constraint to the column radii leaves the problem indeterminate and will result in useless minimum mass designs. For example, packaging requirements or on-orbit handling requirements for most truss applications will impose maximum allowances on the outer radius, r_p . This additional constraint eliminates the possibility of obtaining infinite radii from a mass minimization routine. However, performing the mass minimization will invariably produce a design in which $r_i = r_o$, or, in other words, one with all of the material in the stiffeners and no central column. This result can be easily deduced by realizing that the most efficient location for the material is in the stiffeners, because they are at a greater distance from the centroid than the central column. Likewise, it should be apparent that applying a maximum constraint to any of the radii will give the same minimum mass design result, $r_i = r_o$. Therefore, in order to produce useful minimum mass designs it is necessary to supply two independent constraints on the column radii. Thus, the design procedure consists of seven independent constraint equations and seven independent unknown parameters.

This statement should be alarming because it implies that it is possible to locate the minimum of a parameter in a fully determined system. However, mass minimization considerations form the basis of the derivation of the remaining design condition dealing with stiffener stability. Therefore, the resulting determinate system will, implicitly, describe the minimum mass design.

2.2 Analysis of Stiffener Local Buckling

The discussion in the introduction defined the need for a relationship between the geometric design parameters of the stiffened column and the critical stress for stiffener local buckling. The stiffener is represented as a long slender curved panel of constant radius, and the loading condition that produces stiffener local buckling is uniform axial compression (see Fig. 2.3). The applicable boundary conditions for this problem were determined to be a clamped connection along one of the stiffener's generators and free along the other. Furthermore, it was established that an explicit empirical expression would be more useful for implementation in a design routine than the complex transcendental eight-order system of equations that would be derived from an exact solution of the governing differential equations. This section presents a preliminary discussion of explicit expressions derived for related problems to give insight into the functional

dependence of stiffener local buckling on the geometric design parameters. Finally, the section concludes with the derivation of an explicit empirical expression relating stiffener local buckling stress to the geometric design parameters.

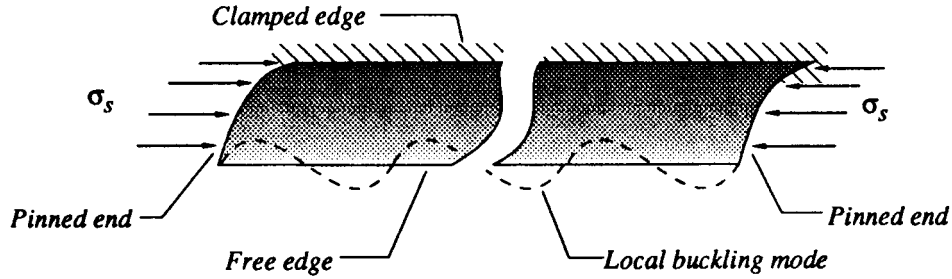


Figure 2.3. Stiffener local buckling mode due to uniform axial compression.

2.2.1 Functional Dependence of Stiffener Local Buckling on Geometric Design Parameters

The six geometric design parameters being considered for the stiffened column (l , r_i , r_o , r_p , ϕ , and ψ) were defined in the previous section. However, the analysis of stiffener local buckling only depends on four of these (l , r_o , r_p , and ψ), because the central column geometry and orientation of the stiffener with respect to the central column have no effect on stiffener local buckling. This result leads to the assumption that the stiffener hinge line can be represented as a clamped connection for the stiffener stability analysis. An equivalent, and more convenient set of geometric parameters for use in studying stiffener local buckling are l , r_s , t_s , and ψ . Where r_s and t_s are the mean radius and thickness of the stiffener and are defined as:

$$r_s = \frac{r_p + r_o}{2} \quad , \quad t_s = r_p - r_o \quad (2.10)$$

In reference 14, Timoshenko and Gere derived expressions for the buckling stress of flat and curved panels, pinned at both ends and acted on by uniform axial compression, for a variety of boundary conditions on both generator edges. These expressions provide explicit relationships between the critical stress and the panel geometric parameters (r_s , t_s , l ,

and ψ for a curved panel and b , t , and l for a flat panel). Although, reference 14 does not address the solution of curved panel stability for the boundary conditions of the present problem, the explicit relationships derived for similar problems provide insight as to the form of an explicit expression for the present problem.

Results from reference 14 indicate that long, slender flat panels ($b \ll l$) restrained by clamped boundaries along one or both of the generator edges tend to buckle as infinitely long panels. In other words, the buckling mode will include a large number of sine waves along the length of the panel, and, consequently, the value of the buckling stress is independent of panel length, l . Since all practical stiffened column designs will be very slender and thus, the stiffeners will be characterized by $r_s \psi \ll l$, it seems reasonable that the stiffener buckling stress will also be independent of column length.

Also, results from reference 14 show that the buckling stress of curved panels tends to be a polynomial function of the non-dimensional quotient, t_s/r_s , regardless of the panel size or boundary conditions. Therefore, it follows that the explicit expression sought herein for the local buckling of curved stiffeners will, most probably, only be a function of two independent geometry parameters, t_s/r_s and ψ .

Another observation from the work presented in reference 14 is that there are a number of different exact expressions for critical stress of a curved panel derived for a given set of boundary conditions. These different expressions only apply within distinct ranges of the geometry parameters, t_s/r_s and ψ . Therefore, it is very important to determine the ranges of these parameters applicable to a particular problem so that the proper expression may be applied. This observation also has significance in the derivation of an approximate empirical expression for stiffener local buckling. Since this expression is to be derived from a matrix of parametric data, it is important to first define the ranges for t_s/r_s and ψ by determining bounding values of these parameters that would be expected in design applications.

It is easy to establish an absolute range for ψ , the stiffener arc angle, as $0 \leq \psi \leq 2\pi/3$ (see Fig. 2.2). However, it should also be noted that there exists a practical lower limit to the arc angle, such that below this limit the structural improvement offered by the stiffeners

is offset by the cost, in complexity and mass, of incorporating the hinged attachments. The preliminary nature of this design study makes it difficult to assess these costs and set a definite value for this lower limit. However, a lower limit of $\pi/3$ will be assumed for generating parametric data leading to an explicit expression for stiffener critical stress, thus, ψ will be bounded as shown in Eq. 2.11.

$$\frac{\pi}{3} \leq \psi \leq \frac{2\pi}{3} \quad (2.11)$$

It is more difficult to set limits on the range of the parameter t_s/r_s . It must be recalled here that the explicit expression for stiffener local buckling is sought as a means of establishing a stiffened column design condition which would result in a minimum mass design having the same values for both stiffener local buckling stress and Euler buckling stress. Therefore, the values of t_s/r_s that would characterize this design boundary for all perceived stiffened column applications can only be determined by understanding this design condition.

This lack of a priori knowledge about the possible range for t_s/r_s necessitates the use of an iterative approach to determine this range. This iterative approach involves making an initial guess for the applicable range of t_s/r_s , and generating parametric data throughout this range from which a design condition could be derived and, consequently, the range for t_s/r_s could be refined. This approach can be applied on subsequent iterations until the bounding values of this range converge. Furthermore, it is possible to use the explicit expression for critical stress of a related problem, a slender flat panel clamped along one generator and free along the other, to determine an initial guess for the range of t_s/r_s . The design condition derived from this range of empirical data can then be used, as stated, to verify or modify the range of t_s/r_s .

Timoshenko and Gere (14) derived the explicit relationship for the local buckling stress of a slender flat panel, clamped along one generator edge and free along the other, and this expression is given in Eq. 2.12. It should be apparent that the critical stress for a curved stiffener is greater than the critical stress of a flat stiffener having the same width and length because of the higher lateral bending stiffness of the curved stiffener. Preliminary numerical stability analyses performed on curved stiffeners indicates that, in

most cases, the critical stress of a curved stiffener is roughly two orders of magnitude greater than that of the flat stiffener. So, a reasonable approximation to the local buckling stress of a curved stiffener is given by Eq. 2.13, where the flat panel width, b , has been replaced by the equivalent curved panel width, $r_s \psi$.

$$\sigma_s = 1.328 E \left(\frac{t_s}{b} \right)^2 \quad (2.12)$$

$$\sigma_s \cong 132.8 E \left(\frac{t_s}{r_s \psi} \right)^2 \quad (2.13)$$

The other equation needed to construct the aforementioned minimum mass design condition is the expression for the Euler buckling stress, σ_e , of the stiffened column. This expression can be determined from Eq. 1.1 by recognizing that the equivalent cross-sectional moment of inertia is equal to the cross-sectional area times the radius of gyration, ρ , squared (Eq. 2.14). The resulting expression is given in Eq. 2.15.

$$I = \rho^2 A \quad (2.14)$$

$$\sigma_e = \pi^2 E \left(\frac{\rho}{l} \right)^2 \quad (2.15)$$

As mentioned previously, a practical stiffened column design would have Euler buckling as its fundamental stability mode. The minimum mass design condition is derived by equating the Euler buckling stress with the stiffener local buckling stress. Applying the expressions in Eq. 2.13 and 2.15 gives the following approximate minimum mass design condition.

$$\pi^2 E \left(\frac{\rho}{l} \right)^2 = 132.8 E \left(\frac{t_s}{r_s \psi} \right)^2$$

It can be shown that the radius of gyration of the stiffened column is typically within twenty percent of the value of the radius of the stiffener, so assuming that $\rho \cong r$, and simplifying the above expression gives the following approximate minimum mass design condition.

$$0.27 \psi \frac{r_s}{l} = \frac{t_s}{r_s} \quad (2.16)$$

It is now possible to define an approximate range for the non-dimensional parameter t_s/r_s by specifying the minimum and maximum values for the parameters ψ , and r_s/l . Eq. 2.11 established a range for the stiffener arc angle, ψ , and an appropriate range for r_s/l may be specified by considering the dimensions of slender columns currently being considered for large space structure applications. A lower bound for r_s/l is represented by the candidate truss components for the Space Station Freedom discussed in reference 22. The diagonal members of this truss have an $r_s/l \cong .0035$. An upper bound for r_s/l is represented by the candidate truss components for the Precision Segmented Reflector testbed structure discussed in reference 23. The members of this truss have an average $r_s/l \cong .016$. Therefore, by applying the minimum and maximum bounds of r_s/l and ψ , respectively, to Eq. 2.15, an approximate range for t_s/r_s is defined to be:

$$.001 \leq \frac{t_s}{r_s} \leq .01 \quad (2.17)$$

2.2.2 Derivation of Approximate Explicit Relationship for Stiffener Local Buckling

As indicated, stiffener local buckling should only be a function of two independent parameters, t_s/r_s and ψ , and Eq. 2.11 and 2.17 define approximate ranges for these parameters that are applicable to the present problem. Therefore, it is now possible to conduct a parametric study to determine an approximate explicit relationship for stiffener local buckling based on local buckling analysis of a large set of stiffeners having dimensions falling within the bounds set in Eq. 2.11 and 2.17.

In the introduction, it was explained that the present study will employ the VIPASA structural analysis routine to generate an efficient linked-plate representation of the structure for numerical solution of the stability problem. As explained, this method of structural representation assumes lengthwise sinusoidal deformations of the structure, and thus requires that only the cross section of the structure be discretized. Fig. 2.4 shows a typical curved stiffener as represented in VIPASA. The constant radius curvature of the stiffener

is approximated with eight discrete flat plate strips. The dashed line in Fig. 2.4 shows the lateral deformation corresponding to a typical stiffener local buckling mode. As stated, the magnitude of this deformation varies sinusoidally along the length of the stiffener with essentially the same wavelength as that for an infinitely long stiffener.

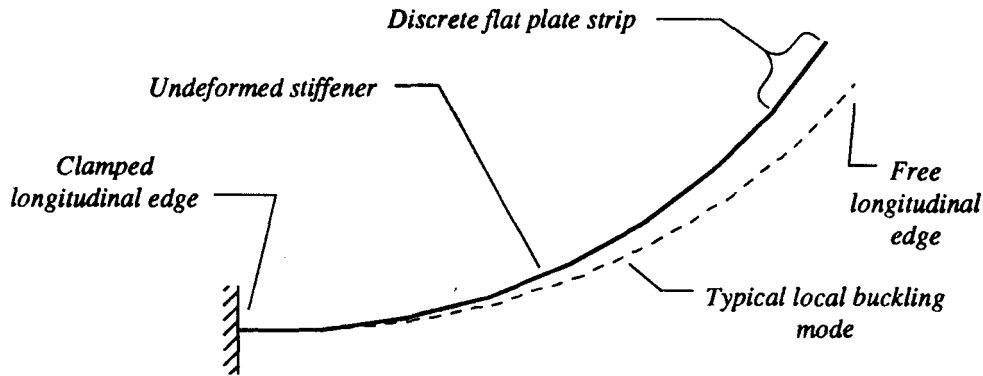


Figure 2.4. Typical plot of curved stiffener as represented in VIPASA.

Preliminary parametric analyses were performed, using the VIPASA model, to verify that the local buckling stress of the curved stiffener is only a function of ψ and t_s/r_s . Although this data is not presented, indeed, this assumption was found to be true throughout the parametric ranges defined in Eq. 2.11 and 2.17. Therefore, subsequent parametric analysis are performed using a value of one inch for the stiffener radius of curvature, r_s , and thus variations in the parameter t_s/r_s are achieved by varying only the thickness, t_s .

A matrix of values for stiffener local buckling stress can be generated by selecting a set of discrete values for the parameters ψ and t_s/r_s , and performing a VIPASA stability analysis on the resulting family of stiffeners. Table 2.1 presents the values of these stresses normalized to the Young's modulus of the stiffener for a family of thirty designs. By reviewing this data, it is apparent that the local buckling stress monotonically increases with increasing t_s/r_s , and decreasing ψ . Furthermore, the corresponding rates of increase of the local buckling stress are approximately constant for both parameters.

Table 2.1. Matrix of Normalized Stiffener Local Buckling Stresses From VIPASA Analysis.

	$\frac{\sigma_s}{E} \times 10^6$, for $t_s/r_s =$					
ψ	0.001	0.002	0.004	0.006	0.008	0.010
$\pi/3$	48.9	150.	317.	500.	697.	909.
$5\pi/12$	32.0	121.	309.	477.	649.	837.
$\pi/2$	24.2	87.4	297.	463.	631.	803.
$7\pi/12$	16.7	65.4	245.	449.	623.	797.
$2\pi/3$	12.7	50.6	195.	411.	603.	774.

This result indicates that a reasonable approximate expression for the normalized local buckling stress might be a bilinear equation in ψ and t_s/r_s . The general form for this bilinear equation is given in Eq. 2.18, where the coefficients b_1 , b_2 , b_3 , and b_4 are constants.

$$\frac{\sigma_s}{E} = b_1 + b_2 \psi + b_3 \frac{t_s}{r_s} + b_4 \psi \frac{t_s}{r_s} \quad (2.18)$$

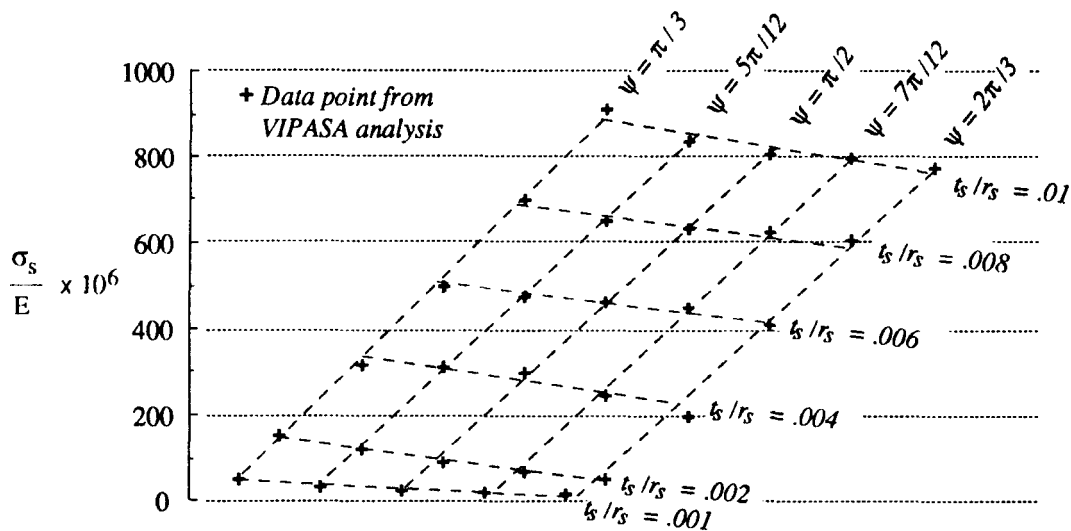


Figure 2.5. Plot of normalized stiffener local buckling stresses from VIPASA analysis.

The data from Table 2.1 is plotted in Fig. 2.5 in the form of a carpet plot, and best-fit interpolation lines corresponding to constant values of ψ and t_s/r_s are dashed in to demonstrate the near linear behavior of the local buckling stress. An important observation from this plot is that the slopes of the lines for the constant values of ψ are very nearly the same. Also, the slopes of the lines for constant values of t_s/r_s are very nearly the same with the exception of the line for $t_s/r_s = 0.001$. Neglecting the case of $t_s/r_s = 0.001$ for the moment, it follows that the local buckling stress should be adequately represented with the planar Eq. 2.19 which is derived from Eq. 2.18 with $b_4 = 0$.

$$\frac{\sigma_s}{E} = b_1 + b_2 \psi + b_3 \frac{t_s}{r_s} \quad (2.19)$$

Considering now the case of $t_s/r_s = 0.001$, it is noted that these data points correspond to very low local buckling stresses and would not be accurately predicted with a planar expression of the form in Eq. 2.19. Results of design studies to be presented in the following chapter will demonstrate that practical stiffened column designs will exhibit buckling stresses above these values. Therefore, a planar expression for local buckling stress will prove sufficiently accurate for the applications being considered.

The method of least-squares (see reference 24) is selected for calculating the coefficients b_1 , b_2 , and b_3 in Eq. 2.19 given the set of discrete data in Table 2.1. Application of this method results in a system of three linear algebraic equations in b_1 , b_2 , and b_3 . This system is given in Eq. 2.20 in which the summation index i denotes the i^{th} data point in Table 2.1, and N is the total number of data points.

$$\begin{bmatrix} N & \sum_{i=1}^N \psi_i & \sum_{i=1}^N \left(\frac{t_s}{r_s}\right)_i \\ \sum_{i=1}^N \psi_i & \sum_{i=1}^N \psi_i^2 & \sum_{i=1}^N \psi_i \left(\frac{t_s}{r_s}\right)_i \\ \sum_{i=1}^N \left(\frac{t_s}{r_s}\right)_i & \sum_{i=1}^N \psi_i \left(\frac{t_s}{r_s}\right)_i & \sum_{i=1}^N \left(\frac{t_s}{r_s}\right)_i^2 \end{bmatrix} \begin{bmatrix} b_1 \\ b_2 \\ b_3 \end{bmatrix} = \begin{bmatrix} \sum_{i=1}^N \left(\frac{\sigma_s}{E}\right)_i \\ \sum_{i=1}^N \left(\frac{\sigma_s}{E}\right)_i \psi_i \\ \sum_{i=1}^N \left(\frac{\sigma_s}{E}\right)_i \left(\frac{t_s}{r_s}\right)_i \end{bmatrix} \quad (2.20)$$

Because Eq. 2.20 is only a third-order system, the solutions for b_1 , b_2 , and b_3 are most easily derived by Gauss elimination and back substitution. Implementing this procedure in a computer program produces the appropriate values of b_1 , b_2 , and b_3 . After substitution of these values into Eq. 2.19, the approximate, explicit expression for stiffener local buckling stress becomes:

$$\sigma_s = E \left(6.0 \times 10^{-5} - 8.74 \times 10^{-5} \psi + 8.97 \times 10^{-2} \left(\frac{t_s}{r_s} \right) \right) \quad (2.21)$$

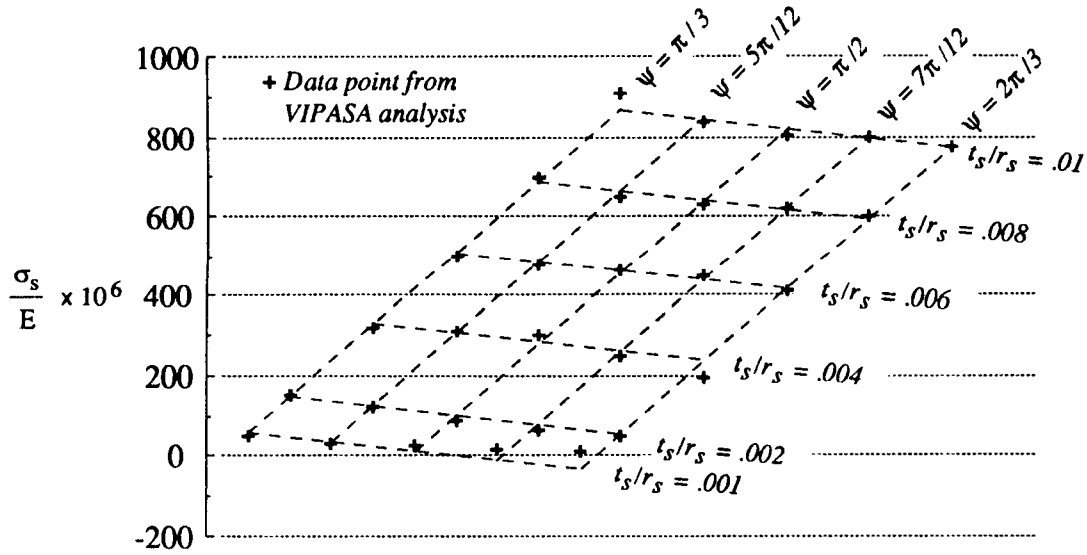


Figure 2.6. Comparison of normalized stresses from VIPASA and explicit expression.

Fig. 2.6 presents a comparison of the stresses predicted using Eq. 2.21 and those from the VIPASA analysis, summarized in Table 2.1. The difference between Fig. 2.6 and Fig. 2.5 is that the dashed lines in Fig. 2.6 are the best-fit planar representation of the stresses derived from Eq. 2.21. As anticipated, the agreement between the approximate stresses and the VIPASA results is quite good with the exception of the very low stress region of the graph where $t_s/r_s < .002$ and $\psi \geq \pi/2$. In this region Eq. 2.21 predicts negative values for the local buckling stress which is obviously inadmissible. Neglecting the three data points for $t_s/r_s = .001$ and $\psi \geq \pi/2$, the rms error of the remaining values predicted using Eq. 2.21 is only 7.2%. Therefore, it is reasonable to apply Eq. 2.21 to predict the local buckling stress of a curved stiffener unless $t_s/r_s < .002$ and $\psi \geq \pi/2$.

Further studies of local buckling for stiffeners with $t_s/r_s > .01$ show that application of Eq. 2.21 to this region results in local buckling stress values which are consistently low when compared to values from VIPASA analysis. This implies that applying Eq. 2.21 to the design of stiffened columns with stiffeners having $t_s/r_s > .01$ would result in a conservative design, and, thus, one which is guaranteed to exhibit Euler buckling as a fundamental stability mode.

It was stated previously that a minimum mass design is one which exhibits the same critical stress for both Euler column buckling and stiffener local buckling. However, to avoid stability mode interaction and ensure Euler buckling for the fundamental stability mode, stiffened column designs will be sought for which the stiffener local buckling stress is greater than the Euler buckling stress. Thus, equating these stresses provides a limiting condition for stiffened column design. This design condition is given in Eq. 2.22 and is derived from the stress expressions in Eq. 2.15 and 2.21.

$$\pi^2 \left(\frac{\rho}{l} \right)^2 \leq \left(6.0 \times 10^{-5} - 8.74 \times 10^{-5} \psi + 8.97 \times 10^{-2} \left(\frac{t_s}{r_s} \right) \right) \quad (2.22)$$

It was pointed out in the first section of this chapter that, with the addition of this design condition, the procedure for generating a minimum mass stiffened column design is characterized by seven parameters; (r_i , r_o , r_p , ϕ , ψ , I , and A), or, equivalently (r_i , r_s , t_s , ϕ , ψ , I , and A), and is governed by five constraint Eq.; 1.1, 2.6, 2.7, 2.8, and 2.22. It was also demonstrated that it is necessary to specify two additional independent conditions on the radii of the stiffened column in order to make the problem determinate, and solvable for a useful design. The following section will address the selection of these additional conditions for general design problems, and then will define a set of conditions and the resulting design routine to be used in example design problems to demonstrate the potential mass savings offered by the stiffened column concept.

2.3 Column Design Algorithm

A main goal of the present study is to demonstrate the potential mass savings offered by the stiffened column concept. This savings will be quantified by comparing design curves of mass versus buckling load for minimum mass stiffened column designs with the

corresponding design curves for the central column with varying thickness. These curves will allow the comparison of two designs which can be used interchangeably for a given application because they have the same outer radius, length, and buckling load. To generate these design curves a design algorithm must be established which solves the determinate system consisting of Eq. 1.1, 2.6, 2.7, 2.8, and 2.22 and two additional conditions on the column radii.

In general, when developing a stiffened column design routine there are a variety of independent conditions on the column radii that can be chosen, and the most useful ones depend on the particular application. For example, it was noted previously that often a maximum value for r_p will be given from packaging or on-orbit handling considerations. Also, manufacturing and handling requirements impose minimum values on wall thickness for both the central column ($r_o - r_i$) and the stiffeners ($r_p - r_o$ or, equivalently, t_s). Alternately, it may be desirable to implement curved deployable stiffeners on a fixed central column design. In which case, both r_i and r_o would be defined, and, thus provide the additional design conditions needed.

In the present study, the later of these additional radius constraints are employed so that mass penalty as a function of increased buckling load can be studied for a fixed central column design. This approach is taken because it is well suited for demonstrating the potential mass savings offered by the stiffened column. A family of minimum mass stiffener designs will be generated for the given central column which have optimum values of t_s , ψ , and ϕ , and, thus, the minimum total column mass, for a range of values of the buckling load. The resulting mass versus buckling load curve will show the minimum percent increase of mass necessary to achieve a particular percent increase in buckling load. As mentioned, the mass savings of the stiffened column will be quantified by comparing this curve to the corresponding mass versus buckling load curve derived for a simple circular column having the same outer radius and buckling load.

By selecting values for r_i and r_o , and defining the buckling load, P_{cr} , it should be obvious that the determinate system describing the minimum mass stiffened column reduces to a five equation (eqs. 1.1, 2.6, 2.7, 2.8, and 2.22) and five unknown (t_s , ϕ , ψ , I , and A) system. Furthermore, it can be seen that Eq. 1.1 and 2.7 and the variables, I and A uncouple, and leave a three by three system to be solved. However, reviewing the

remaining equations, it is seen that this system is highly coupled and nonlinear, thus difficult to solve. An alternate approach to solving this system is to select the value for ψ at the outset, and allow the buckling load, P_{cr} , to become a solution variable. This approach results in a relatively simple iterative solution procedure for the nonlinear system, which will be shown to converge quite quickly to the desired system solution.

The first step in developing this solution procedure is to rearrange Eq. 2.22 by solving for t_s . The resulting expression is given in Eq. 2.23.

$$t_s \geq r_s \left(1.10 \times 10^2 \left(\frac{\rho}{l} \right)^2 + 9.74 \times 10^{-4} \psi - 6.69 \times 10^{-4} \right) \quad (2.23)$$

Eq. 2.23 appears to be an explicit expression for t_s , however r_s and ρ are both implicit functions of t_s through the remaining system equations and Eq. 2.10 and 2.14 (recall that ψ has been defined at the outset). Therefore, Eq. 2.23 is in the correct form for application of fixed-point iteration to determine the solution for t_s (see reference 24). This iteration procedure is quite simple. An initial estimate for t_s is made and substituted into the right hand side of Eq. 2.23, then the equation is solved to determine the new estimate for t_s , and this procedure is repeated until t_s converges. At each iteration step, the new values for r_s and ρ are calculated from Eq. 2.6, 2.7, 2.8, 2.10, and 2.14 which uncouple if solved in the order: 2.8, 2.6, 2.7 then 2.10 and 2.14.

Rather than making an initial estimate for t_s and solving the system of equations for initial estimates of r_s and ρ , it is easier to begin the iteration process by making initial estimates for r_s and ρ . These initial values are assumed to be the outer radius of the central column, r_o . Although this initial estimate implies that $t_s = 0$ (from Eq. 2.10) it will be shown that the fixed-point iteration procedure will, nonetheless, converge rapidly to the desired solution.

By determining a converged solution for t_s , converged solutions for r_s , ϕ , ρ , I , and A are also implicitly determined using this process. Finally, the value for buckling load, P_{cr} , can be determined from the value of I , and Eq. 1.1. Therefore, the result of this iteration procedure is the minimum mass design and the corresponding buckling load of a stiffened

column having a stiffener arc angle = ψ .

A complete curve of minimum column mass versus buckling load can be generated by determining minimum mass design for the complete range of ψ . It will be shown that as ψ is increased, so will the minimum mass and buckling load of the column. Finally using Eq. 1.1, 2.5 and 2.7 with $I_{sa} = \psi = 0$, it is possible to calculate a set of masses and buckling loads of the central column for a range of thicknesses.

Appendix B presents a flow chart and a listing of the FORTRAN computer program DESTCO that was written to perform the fixed-point iterative solution of the above system of equations, and generate the mass versus buckling load design curve data for both the minimum mass stiffened column and the central column. The program was written and executed using a FORTRAN compiler on a desk-top personal computer.

CHAPTER 3

EXAMPLES AND DISCUSSION

This chapter is a summary of results from stiffened column design studies conducted using the design program DESTCO. These studies will serve to illustrate the procedures involved in generating minimum mass stiffened column designs, as well as verify that the resulting designs exhibit Euler buckling as their fundamental stability mode. The first section of the chapter presents two stiffened column design examples which are applicable to typical large space structure missions currently envisioned and analyses to verify the DESTCO results. The final section presents a discussion of the results, and additional practical considerations for implementation of stiffened column designs.

3.1 Generation of Design Curves for Example Problems

In the last chapter it was explained that the design routine embedded in the DESTCO program requires that the central column size be completely specified (r_i , r_o , and l). Therefore, application of this routine results in the set of minimum mass curved stiffeners for the given central column and the corresponding values for percent increase in column buckling load and mass.

Two example central column designs have been selected for illustrative purposes in generating minimum mass stiffener designs. The first is from the Space Station Freedom five-meter truss structure (see reference 22), and the second is from the Precision Segmented Reflector two-meter truss structure (see reference 23). The nominal dimensions assumed for these two central columns are given in Table 3.1.

Table 3.1. Nominal Dimensions for Example Central Columns.

Example Column	r_i (in)	r_o (in)	l (in)
Space Station Freedom	0.9675	1.0325	196.8
Precision Segmented Reflector	0.4700	0.5300	78.7

The dimensions in Table 3.1 are used as input to DESTCO to generate the set of minimum mass stiffener designs for the range of stiffener arc angles given in Eq. 2.11. Tables 3.2 and 3.3 present these results for the Space Station Freedom column and the Precision Segmented Reflector column, respectively.

Table 3.2. Design Data for Space Station Freedom Column.

ψ	t_s (in)	t_s / r_s	Φ (deg)	I (in ⁴)	A (in ²)
$\pi/3$.0019	.0018	110.	.212	.415
$5\pi/12$.0022	.0021	115.	.217	.417
$\pi/2$.0025	.0024	120.	.225	.420
$7\pi/12$.0028	.0027	125.	.235	.424
$2\pi/3$.0031	.0030	129.	.248	.429

Table 3.3. Design Data for Precision Segmented Reflector Column.

ψ	t_s (in)	t_s / r_s	Φ (deg)	I (in ⁴)	A (in ²)
$\pi/3$.0014	.0026	110.	.0244	.191
$5\pi/12$.0016	.0029	115.	.0249	.192
$\pi/2$.0017	.0032	120.	.0256	.193
$7\pi/12$.0019	.0036	125.	.0264	.194
$2\pi/3$.0021	.0039	129.	.0275	.195

It should be recalled that the empirical expression for stiffener local buckling derived in the last chapter (eq. 2.21) is only applicable for the range $.001 \leq t_s/r_s \leq .01$ with the exception of $.002 \leq t_s/r_s$ when $\psi \geq \pi/2$. Initial approximate stiffener local buckling analyses determined these bounds as appropriate for typical stiffened column design problems to be considered. Fig. 3.1 shows the actual variation in t_s/r_s for the minimum mass designs of the two examples considered. It is seen that, indeed, these designs all lie within the aforementioned bounds on t_s/r_s , and thus, the analyses imbedded in the DESTCO program are applicable to these examples.

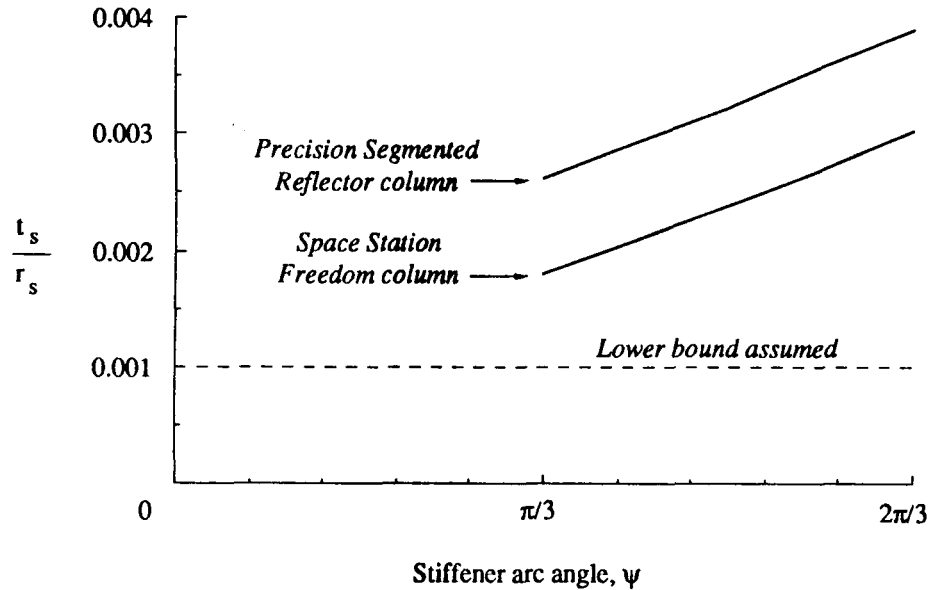


Figure 3.1. Stiffener thickness variation with arc angle for minimum mass designs.

It is important that the designs generated using DESTCO have values for t_s/r_s which are within the acceptable limits. If not, one could either derive a new stiffener local buckling expression, applicable for the new range, or one could use the original results and accept the lower solution accuracy. Recall that the error in employing the DESTCO program outside of the specified range on t_s/r_s , should result in only near-minimum mass designs, but the fundamental stability mode of these designs should still be Euler buckling.

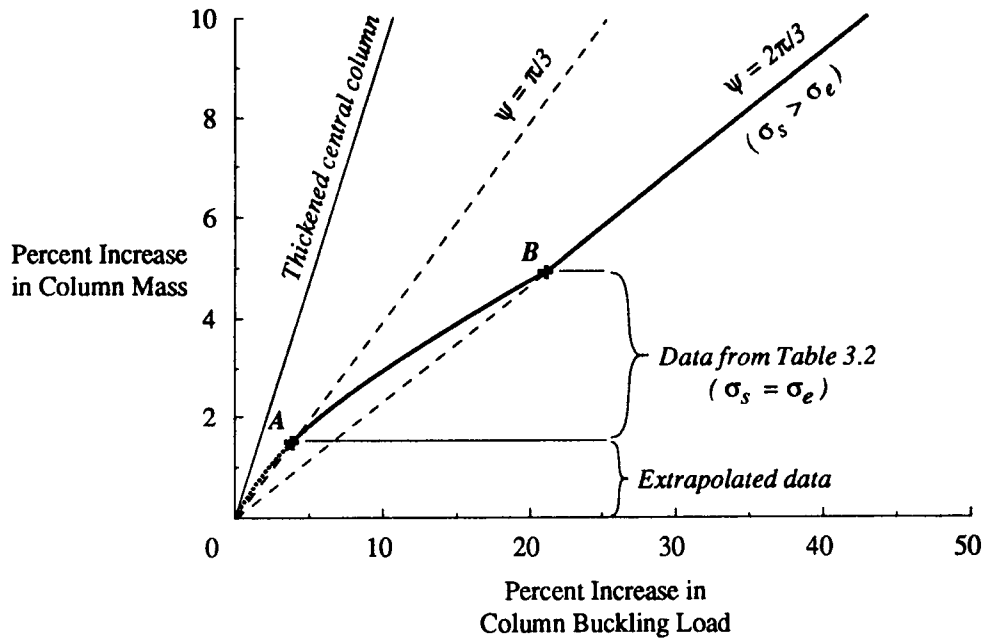


Figure 3.2. Minimum mass design curve for Space Station Freedom column.

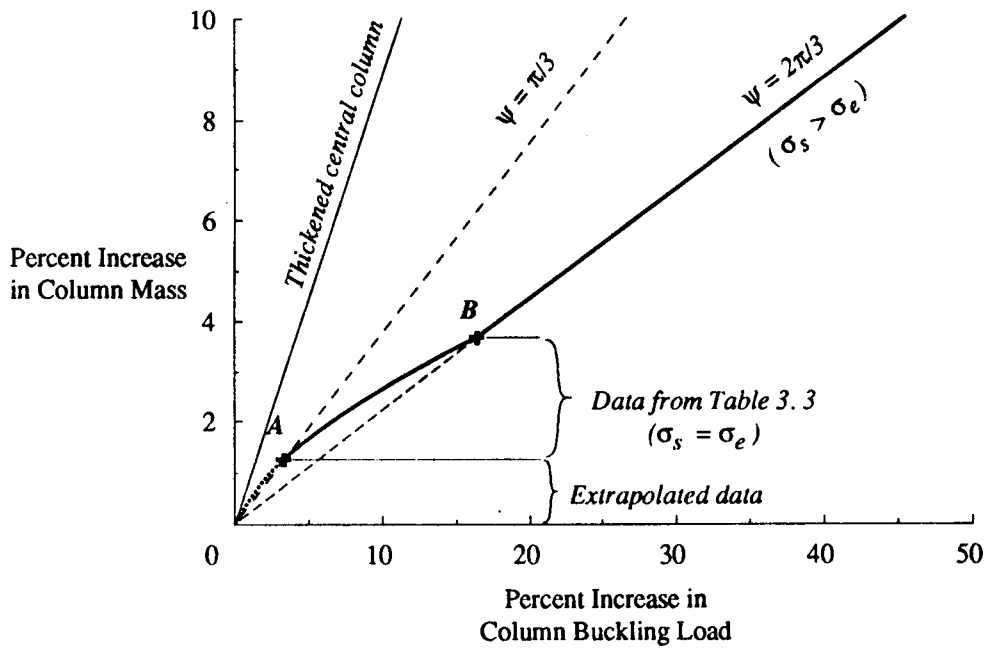


Figure 3.3. Minimum mass design curve for Precision Segmented Reflector column.

The minimum mass designs presented in Tables 3.2 and 3.3 represent the stiffener thickness, for a given stiffener arc angle, that results in equal Euler buckling and stiffener local buckling stresses (see Eq. 2.23). Designs with larger thicknesses will have Euler buckling as their fundamental stability mode, and designs with smaller thicknesses will have stiffener local buckling as their fundamental stability mode. Additionally, for designs which behave as Euler columns, the percent increases in buckling load and mass are equal to the percent increases in cross-sectional inertia and area, respectively. Therefore, the data in Tables 3.2 and 3.3 can be used to generate a portion of a stiffened column design curve showing minimum percent mass increase versus percent buckling load increase.

Fig. 3.2 and 3.3 show the complete minimum mass design curves for the Space Station Freedom column and the Precision Segmented Reflector column, respectively. The two dashed lines superimposed over these curves represent stiffened columns having stiffener arc angles of $\pi/3$ and $2\pi/3$ and are generated using Eq. 2.6 and 2.7 with successively increasing values of stiffener thickness. The portion of the design curve between the origin and point *B* represents designs with increasing values of stiffener thickness and arc angle, for which the Euler buckling stress equals the stiffener local buckling stress. The portion of the curve between points *A* and *B* was generated from data in Tables 3.2 and 3.3, and is extrapolated to the origin to show an approximation of the curve in this region. The portion beyond point *B*, represents designs having $\psi=2\pi/3$ (the imposed upper limit on stiffener arc angle) and increasing stiffener thicknesses. As mentioned, designs in this region have Euler buckling stresses which are less than their stiffener local buckling stresses.

The lighter weight solid lines in Fig. 3.2 and 3.3 show the mass penalty necessary to get the given buckling load increase by simply increasing the thickness of the central column. These lines are generated using Eq. 2.5 and 2.7. The difference between the thickened central column line and the minimum mass design curve is the mass savings attributed to the stiffened column concept. The slope of the thickened central column line is approximately one. This follows from the fact that, for a thin circular cross section, both the inertia and the area are proportional to the thickness, and thus, a given increase in thickness will cause the same percent increase in both area and inertia. Conversely, the slope of the minimum mass design curve beyond point *B* is approximately 1/4, and thus, a

given percent increase in buckling load in this region, will require only 1/4 of that percentage in increased mass.

The design curves in Fig. 3.2 and 3.3 can be verified through further analysis. As mentioned, the portion of the curves between points A and B should represent the boundary between designs with Euler buckling as their fundamental stability mode and designs with stiffener local buckling as their fundamental stability mode. Fig. 3.4 is an exploded view of this portion of the design curve for the Space Station Freedom column. The square data points along the design curve correspond to designs which were analysed using VIPASA and verified to have Euler buckling as a fundamental stability mode. Additionally, models of these designs, with slightly smaller values for stiffener thickness, were analysed and determined to exhibit stiffener local buckling as their fundamental stability mode. These data points are indicated with stars in Fig. 3.4. These results indicate that, indeed, the design curves presented represent the minimum mass designs and the boundary between designs with Euler buckling as their fundamental stability mode and those with stiffener local buckling as their fundamental stability mode.

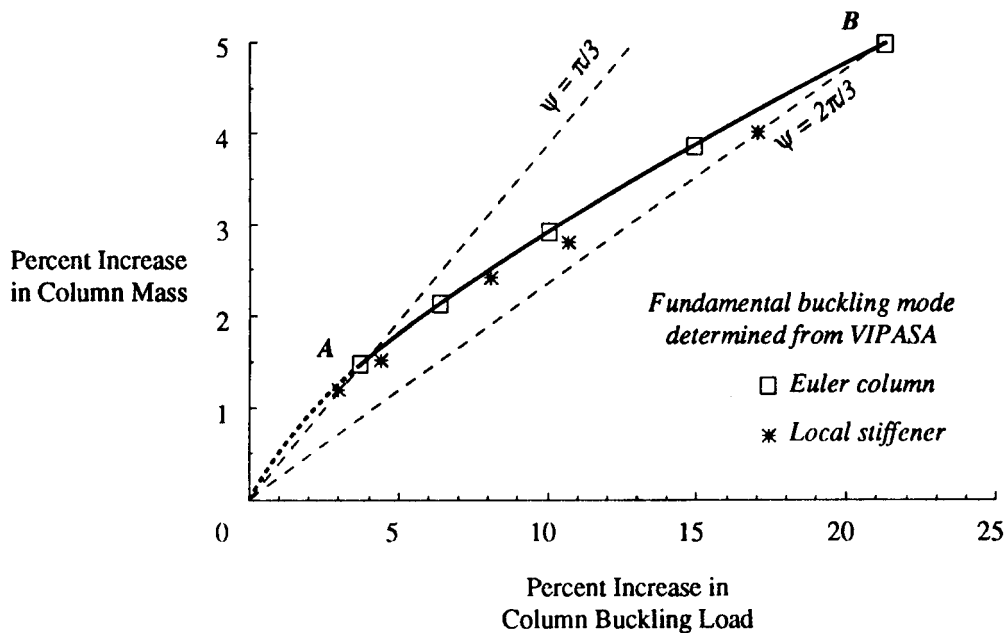


Figure 3.4. Verification of Space Station Freedom column design curve.

3.2 Discussion of Results

It should be reiterated that the design curves presented in Fig. 3.2 and 3.3 present the percent increase in only the structural mass of the stiffened columns, with no allowance for the added mass of the hinge and deployment mechanisms attaching the stiffeners to the central column. This added mechanism mass can be estimated as a percentage of the mass of the central column, and can be considered a constant for the entire range of stiffener designs. Fig. 3.5 shows the minimum mass design curve for the Space Station Freedom column when the mass of the hinge and deployment mechanisms is assumed to be 10 percent of the central column mass. This curve is constructed by simply adding 10 percent to the minimum mass design curve in Fig. 3.2.

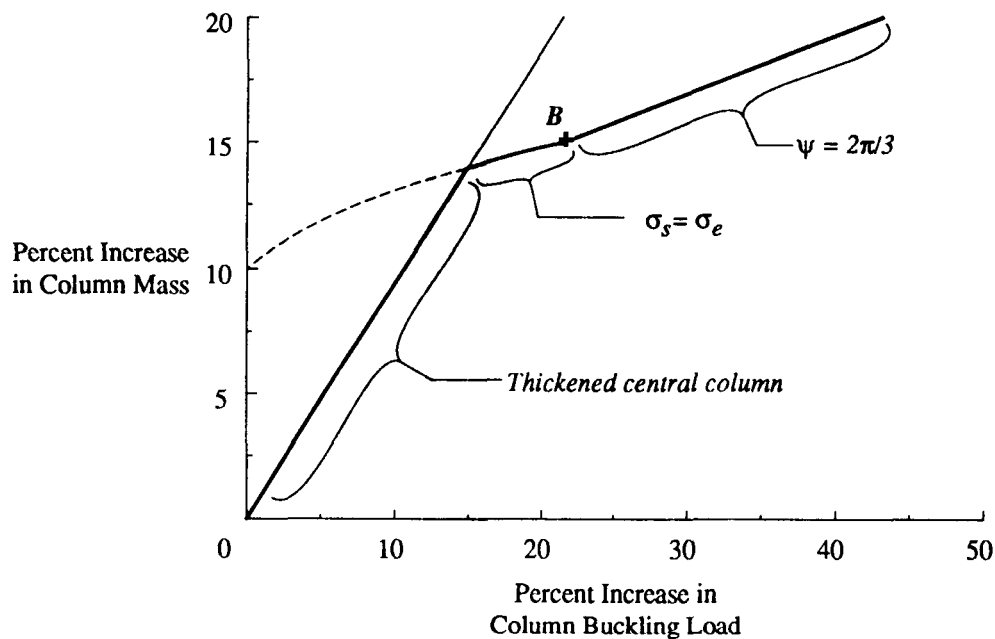


Figure 3.5. Design curve for Space Station Freedom column including 10% mechanism mass.

It is apparent from this figure that the added mechanism mass significantly changes the character of the minimum mass design curve. When mechanism mass is considered, small to moderate increases in buckling load can be achieved with less mass penalty by simply increasing the wall thickness of the central column. In this example, buckling load increases up to about 15 percent would favor the thickened central column over the central

column with deployable stiffeners. Also, this cross over point occurs fairly close to point *B* which is the start of the portion of the design curve on which $\psi=2\pi/3$. This implies that the addition of an appreciable mechanism mass causes the region of the design curve between points *A* and *B* in Fig. 3.2 and 3.3 to become essentially unimportant. Thus the consideration of stiffener local buckling is unnecessary. Therefore the practical column design problem is reduced to the consideration of only two design regions: thickened central column for low buckling load increases and stiffened column with $\psi=2\pi/3$ for higher buckling load increases.

The upper and lower portions of the design curve in Fig. 3.5 are generated using Eq. 2.5, 2.6 and 2.7, and by linearly increasing the value of stiffener thickness (upper portion of curve) or central column thickness (lower portion of curve). The near linear shape these segments of the curve suggest that Eq. 2.5, 2.6 and 2.7 may be linearized with respect to these two thicknesses and still give accurate results. Performing this linearization is exactly equivalent to invoking the following small thickness assumptions.

$$\begin{aligned}(r_i + r_o) &\approx (r_o + r_p) \approx 2r \\ t_{cc} &= r_o - r_i \ll r \\ t_s &= r_p - r_o \ll r\end{aligned}\tag{3.1}$$

Additionally, a further simplification can be made by observing a result presented in reference 12. In this reference, it was demonstrated that the cross-sectional inertia of the stiffened column does not vary more than five percent for deployment angles within 10 to 15 degrees of the optimum value. Therefore, it is possible to assume the deployment angle, $\phi = 2\pi/3$ and still ensure a reasonable approximate result. Applying this assumption and the small thickness assumptions in Eq. 3.1 to Eq. 2.5, 2.6 and 2.7 gives the following linearized equations governing the design of a thickened central column and a stiffened column with $\psi=2\pi/3$.

$$I_{cc} \equiv \pi r^3 t_{cc} \tag{3.2}$$

$$I \equiv \pi r^3 (t_{cc} + 4t_s) \tag{3.3}$$

$$A \cong 2\pi r(t_{cc} + t_s) \quad (3.4)$$

These equations illustrate the conclusions previously drawn. First, an increase in thickness of the central column will cause the same percent increase in both area and inertia. Second, an increase in thickness of the stiffeners will give rise to a percent increase in inertia which is four times the percent increase in area.

Eq. 3.2, 3.3, and 3.4 can be used to generate an approximate stiffened column design curve. Fig. 3.6 presents this approximate design curve superimposed over the exact curve from Fig. 3.5. In this example, the approximate curve is in reasonable agreement with the exact curve. Furthermore, the approximate curve gives consistently conservative results (slightly higher mass increase for a given buckling load increase). Therefore, it is reasonable to simply use the approximate expressions given in Eq. 3.2, 3.3, and 3.4 to generate first iteration design curves.

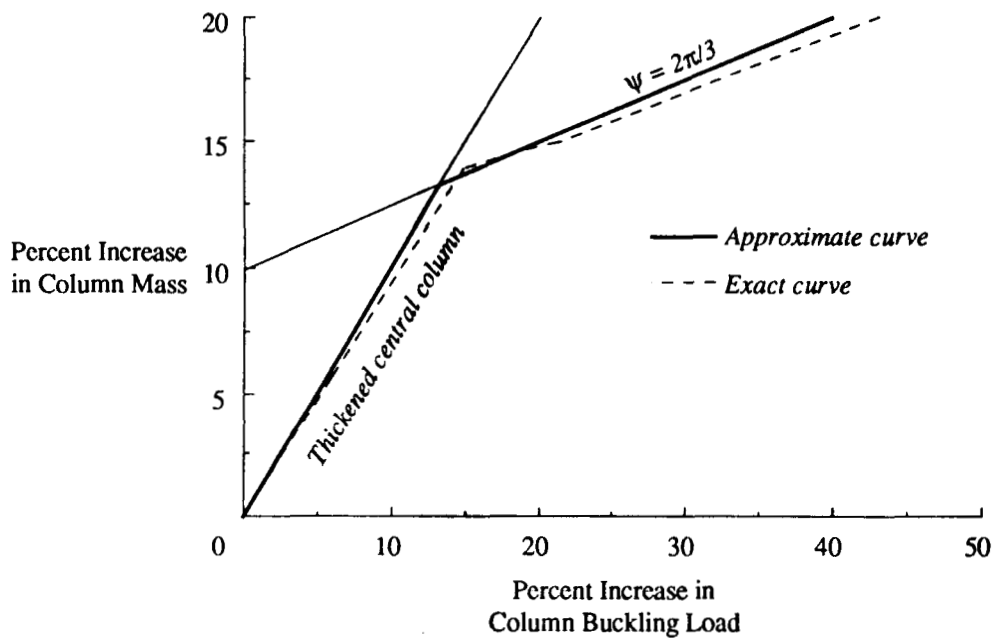


Figure 3.6. Comparison of approximate and exact design curves for Space Station Freedom column including 10% mechanism mass.

It should be noticed that the approximate percent mass increase and buckling load increase are only linear functions of the percent increase in t_{cc} and t_s . Consequently, a general expression can be easily derived from Eq. 3.3 and 3.4 which relates the percent increase in stiffened column mass (ΔM) to the percent increase in buckling load (ΔP_{cr}) and the deployment mechanism mass as a percentage of the central column mass (M_m). This expression is given in Eq. 3.5 and applies to any stiffened column design having $\psi = 2\pi/3$.

$$\Delta M = .25\Delta P_{cr} + M_m \quad (3.5)$$

A family of approximate stiffened column design curves can be generated from Eq. 3.5 using a set of values for the deployment mechanism mass. Fig. 3.7 presents one such family of curves. These curves provide a first iteration estimate of the percent mass increase necessary to achieve a given percent buckling load increase for any stiffened column application.

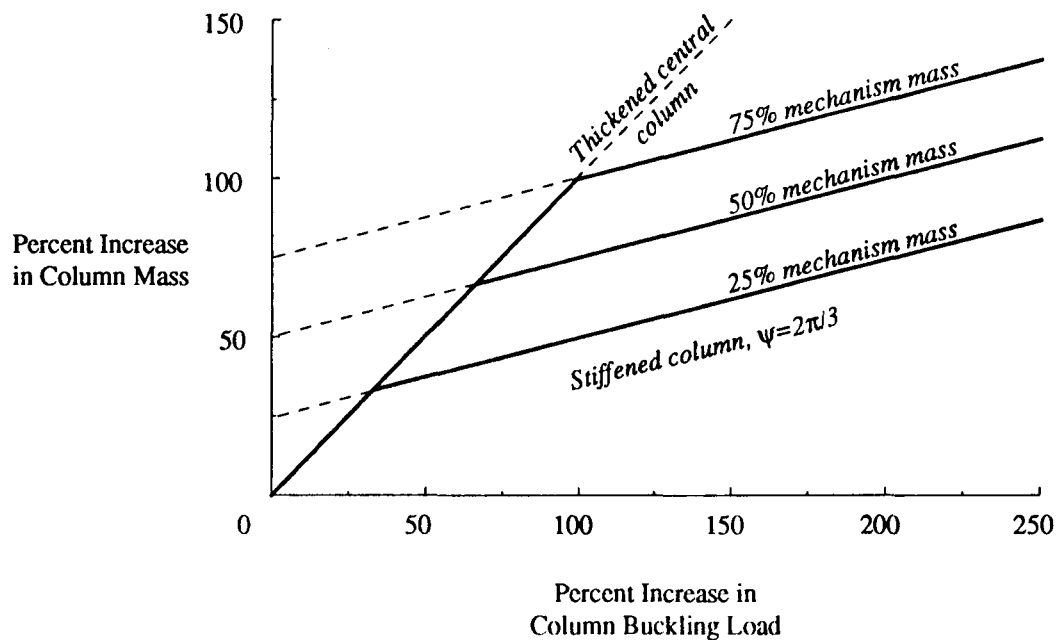


Figure 3.7. Family of approximate general stiffened column design curves.

As an illustrative example, if one desires to increase the buckling load of a circular column by 200 percent using deployable stiffeners, and one assumes that the mass of the deployment mechanism would be 50 percent of the mass of the central column, then Eq. 3.5 and, similarly, Fig. 3.7 shows that this would require approximately a 100 percent increase in total column mass. This compares to a 200 percent increase in total mass if the increased buckling load is achieved through simply thickening the central column.

Finally, for further evaluating the usefulness of stiffened columns, Appendix C presents the effect of deployable stiffeners on column fundamental vibration frequency. The results from these calculations indicate that there is an increase in column vibration frequency with the addition of deployable stiffeners just as there is an increase in column buckling load. However, the percent increase in vibration frequency is typically an order of magnitude less than the percent increase in buckling load, thus deployable stiffeners appear not to be well suited for an application only requiring an increase in vibration frequency.

CHAPTER 4

CONCLUSIONS

This paper has presented the results of a stability design study of a slender column with curved longitudinal stiffeners for large space structure applications. These stiffeners are attached to the central column through deployment mechanisms which allow the stiffeners to package flush around the outside of the central column. The stiffened column concept is attractive because it allows the buckling load of a slender column to be increased at a fairly low cost in increased mass, and with no change to the packaged size of the column. Furthermore, the use of deployable stiffeners eliminates the need for extra on-orbit assembly time which is characteristic of other high-buckling-load, low-packaged-volume column concepts.

The symmetry of the stiffened column cross section gives rise to a zero product of inertia and, consequently, a constant value for moment of inertia regardless of reference axis orientation. Therefore, the stiffened column is perfectly suited for stability applications because it does not have a "preferred" direction of buckling.

The kinematic attachment constraints offered by the stiffener deployment mechanisms are very important in determining the stability modes of the stiffened column. Stiffener attachment mechanisms which do not allow shear load to be transferred may require non-linear numerical analysis to determine stiffener buckling modes. For the purposes of this study, the stiffener attachment is assumed to provide perfect shear load transfer, and thus, the stiffener buckling analysis performed is strictly linear.

An approximate explicit expression describing stiffener local buckling stress was derived from numerical analysis results using a one dimensional "linked-plate" approximation to the stiffener differential equations. This approximate expression was

demonstrated to be accurate to within ten percent for the appropriate range in geometric parameters. Also, equations were derived which relate the set of geometric parameters to column mass and buckling load. The resulting indeterminate system was studied to determine mass minimization considerations. The need for additional geometric constraints was defined, and one set was selected for construction of a determinate minimum mass stiffened column design routine.

The resulting column design routine was used to construct design curves for two current large space structure applications: the Space Station Freedom column and the Precision Segmented Reflector column. These curves are comprised of two segments: one representing designs for which Euler buckling stress equals stiffener local buckling stress and the other representing designs for which the stiffener arc angle is fixed at $2\pi/3$ and Euler buckling stress is less than stiffener local buckling stress. The designs on the first segment of the design curve were verified through further numerical analysis of the entire stiffened column cross section using the "linked-plate" structural representation.

These examples demonstrate that stiffener local buckling is only a concern for stiffened columns having approximately 20 percent or less increase in buckling load over that of the central column. Also, this lower design range proves to be of no practical interest after allowing for the increased mass necessary for the stiffener deployment mechanisms. Therefore, stiffener local buckling proves to not be a concern for practical stiffened column designs. Consequently, the stiffened column design problem is reduced to determining the necessary stiffener thickness and corresponding optimum deployment angle to achieve a given percent increase in cross-sectional inertia.

Furthermore, the equations for cross-sectional inertia and area of the stiffened column can be linearized in terms of the stiffener and central column thicknesses by invoking small thickness approximations. These approximate equations result in a very simple approximate design equation which relates the percent increase in column mass to the percent increase in column buckling load and the stiffener deployment mechanism mass. Neglecting deployment mechanism mass, it turns out that a given percent increase in area of the stiffened column (through increased stiffened thickness) will give rise to four times that percent increase in inertia. This is compared to the mass penalty associated with increasing the buckling load of the central column by simply increasing its thickness. In this case, a

given percent increase in area of the central column will cause only the same percent increase in inertia.

The potential mass savings offered by the stiffened column are clear. In the ideal case where the deployment mechanisms are assumed to add negligible mass, it offers a given buckling load improvement at one fourth the added mass of a circular column with the same outer radius. In practical cases where the deployment mechanisms are known to add a certain amount of mass, the mass savings of the stiffened column are small for small buckling load increases, but approach the ideal rate for higher buckling load increases.

Finally, results from calculations of column fundamental vibration frequency indicate that there is an increase in column vibration frequency with the addition of deployable stiffeners just as there is an increase in column buckling load. However, the percent increase in vibration frequency is typically an order of magnitude less than the percent increase in buckling load, thus deployable stiffeners appear not to be well suited for an application only requiring an increase in vibration frequency.

REFERENCES

1. *Large Space Antenna Systems Technology - 1982, Parts 1 and 2.* NASA CP-2269, November 30-December 3, 1982.
2. *Large Space Antenna Systems Technology - 1984, Parts 1 and 2.* NASA CP-2368, December 4-6, 1984.
3. Mikulas, Martin M., Jr.; Croomes, Scott D.; Schneider, William; Bush, Harold G.; Nagy, Kornell; Pelischek, Timothy; Lake, Mark S.; and Wesselski, Clarence: *Space Station Truss Structures and Construction Considerations.* NASA TM-86338, January 1985.
4. Mikulas, Martin M., Jr.; Bush, Harold G.; and Card, Michael F.: *Structural Stiffness, Strength and Dynamic Characteristics of Large Tetrahedral Space Truss Structures.* NASA TMX-74001, March 1977.
5. Mikulas, Martin M., Jr.; and Bush, Harold G.: *Advances in Structural Concepts.* Published in *Large Space Antenna Systems Technology - 1982, Part 1*, NASA CP-2269 November 30-December 3, 1982, pp. 257-283.
6. Reinert, R. P.: *Weight Optimization of Ultra Large Space Structures.* Presented at the 38th Annual Conference of the Society of Allied Weight Engineers, Inc., May 1979, SAWE paper No. 1301.
7. Heard, Walter L., Jr.; Bush, Harold G.; Walz, Joseph E.; and Rehder, John J.: *Structural Sizing Considerations for Large Space Platforms.* AIAA Journal of Spacecraft and Rockets, Vol. 18, No. 6, Nov.-Dec., 1981, pp. 556-564.
8. Bush, Harold G.; Heard, Walter L., Jr.; Walz, Joseph E.; and Rehder, John J.: *Deployable and Erectable Concepts for Large Spacecraft.* Presented at the 39th Annual Conference of the Society of Allied Weight Engineers, Inc. May 1980, SAWE paper No. 1374.
9. Bush, Harold G.; Heard, Walter L., Jr.: *General Description of Nestable Column Structural and Assembly Technology.* NASA TM-83255, December 1981.
10. Heard, W. L., Jr.; Bush, H. G.; and Agranoff, Nancy: *Buckling Tests of Structural Elements Applicable to Large Space Trusses.* NASA TM-78628, October 1978.
11. Mikulas, Martin M., Jr.: *Structural Efficiency of Long Lightly Loaded Truss and Isogrid Columns for Space Applications.* NASA TM-78687, July 1978.

12. Lake, Mark S.; and Wu, K. Chauncey: *Preliminary Investigation of Stability of a Fin-Stiffened Slender Strut*. NASA TM 4034, April 1988.
13. Donnell, Lloyd Hamilton: *Beams, Plates, and Shells*. McGraw-Hill Book Co., 1976.
14. Timoshenko, Stephen P.; and Gere, James M.: *Theory of Elastic Stability*, Second ed. McGraw-Hill Book Co., 1961.
15. Murray, N. W.: *Introduction to the Theory of Thin-Walled Structures*. Clarendon Press, 1984.
16. Brush, Don O.; and Almroth, Bo O.: *Buckling of Bars, Plates, and Shells*. McGraw-Hill Book Co., 1975.
17. Wittrick, W. H.: *General Sinusoidal Stiffness Matrices for Buckling and Vibration Analyses of Thin Flat-Walled Structures*. International Journal of Mechanical Sciences 1968, Vol. 10, pp. 949-966.
18. Wittrick, W. H.; and Williams, F. W.: *Buckling and Vibration of Anisotropic or Isotropic Plate Assemblies Under Combined Loadings*. International Journal of Mechanical Sciences 1974, Vol. 16, pp. 209-239.
19. Stroud, W. Jefferson; and Anderson, Melvin S.: *PASCO: Structural Panel Analysis and Sizing Code, Capability and Analytical Foundations*. NASA TM-80181, November 1981.
20. Anderson, Melvin S.; Stroud, W. Jefferson; Durling, Barbara J.; and Hennessy, Katherine W.: *PASCO: Structural Panel Analysis and Sizing Code, User's Manual*. NASA TM-80182, November 1981.
21. Roark, Raymond J.; and Young, Warren C.: *Formulas for Stress and Strain*, Fifth ed. McGraw-Hill Book Co., 1982.
22. Mikulas, Martin M., Jr.; and Bush, Harold G.: *Design, Construction and Utilization of a Space Station Assembled from 5-Meter Erectable Struts*. NASA TM-89043, October 1986.
23. Collins, Timothy J.; and Fichter, W. B.: *Support Trusses for Large Precision Segmented Reflectors: Preliminary Design and Analysis*. NASA TM-101560, March 1989.
24. Burden, Richard L.; and Faires, J. Douglas: *Numerical Analysis*, Third ed. PWS-Kent Publishing Co., 1985.

APPENDIX A

DERIVATION OF STIFFENER CROSS-SECTIONAL INERTIAS

The cross-sectional moment of inertia components of the curved stiffener can be calculated for arbitrary stiffener dimensions and deployment angle by performing the appropriate double integrals. The general expressions for these integrals are given in Eq. A.1.

$$I_{sx} = \iint_{\text{cross section}} y^2 dA \quad (\text{A.1})$$

$$I_{sy} = \iint_{\text{cross section}} x^2 dA$$

Before evaluating these integrals, it is necessary to define a convenient coordinate system and appropriate limits for the integrals. Due to the circular curvature of the stiffener cross section, it is convenient to use a polar coordinate system centered at the stiffener's center of curvature. Fig. A.1 shows a stiffener of arc angle ψ at the deployment angle ϕ , with the column cross section oriented such that the stiffener's center of deployment rotation lies along the global y axis. This center of deployment rotation lies along the middle surface through the stiffener's thickness and, for this study, is defined to be a distance away from the edge equal to half the stiffener thickness $((r_p - r_o)/2)$. Integration in polar coordinates will be conducted relative to the local coordinate system (x', y') which is centered at the global coordinates (x_o, y_o) . Eq. A.2 gives the expressions for these global coordinates.

$$x_o = \left(\frac{r_o + r_p}{2} \right) \sin(\phi), \quad y_o = \left(\frac{r_o + r_p}{2} \right) (1 - \cos(\phi)) \quad (\text{A.2})$$

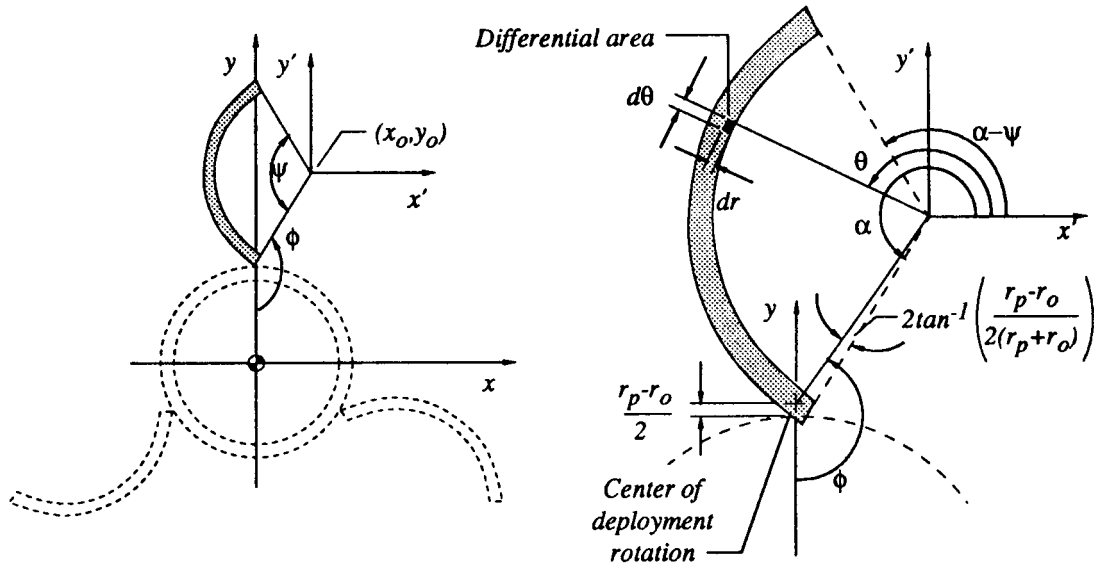


Figure A.1. Cross-sectional parameters for stiffener moments of inertia.

As seen in Fig. A.1, a differential area element can be defined at any angle, θ , and radius, r , relative to the local coordinate system. Also, the global coordinates of this area element are easily defined as in Eq. A.3.

$$\begin{aligned} x &= \left(\frac{r_o + r_p}{2} \right) \sin(\phi) + r \cos(\theta) \\ y &= \left(\frac{r_o + r_p}{2} \right) (1 - \cos(\phi)) + r \sin(\theta) \end{aligned} \quad (\text{A.3})$$

Now it is possible to express the explicit polar form of Eq. A.1. These expressions are given in Eq. A.4. Performing these integrations will result in Eq. 2.3 and Eq. 2.4 given in the main text.

$$\begin{aligned} I_{sx} &= \int_{\alpha-\psi}^{\alpha} \int_{r_p}^{r_o} \left(\frac{r_o + r_p}{2} (1 - \cos(\phi)) + r \sin(\theta) \right)^2 r dr d\theta \\ I_{sy} &= \int_{\alpha-\psi}^{\alpha} \int_{r_p}^{r_o} \left(\frac{r_o + r_p}{2} \sin(\phi) + r \cos(\theta) \right)^2 r dr d\theta \end{aligned} \quad (\text{A.4})$$

APPENDIX B

DESIGN OF STIFFENED COLUMN CODE (DESTCO)

The computer program DESTCO was developed for the design of stiffened columns using design rules developed in the present study. The program was written and executed using a FORTRAN 77 compiler on a desk-top personal computer. Fig. B.1 presents a flow chart which explains program execution, and following is a program listing.

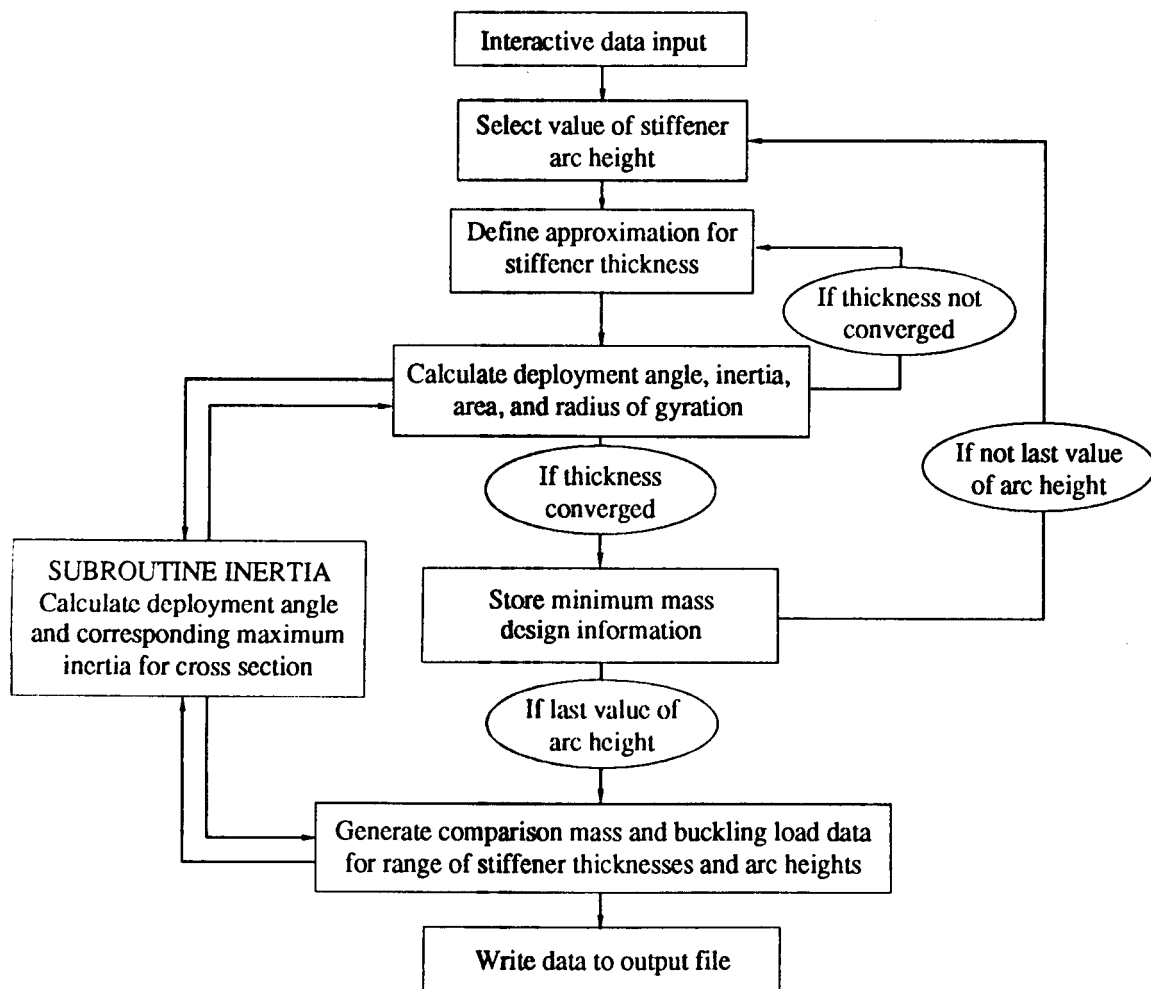


Figure B.1. Flow chart of DESTCO program.

```

C .....
C
C                               D E S T C O
C
C THIS IS A PROGRAM TO GENERATE THE DESIGN CURVE FOR A LATER-
C ALLY STIFFENED SLENDER COLUMN. THE CROSS SECTION INCLUDES A
C CIRCULAR TUBE WITH THREE CYLINDRICAL OPEN SECTIONS FUN-
C CTIONING AS DEPLOYABLE STIFFENERS WHICH INCREASE THE BENDING
C STIFFNESS OF THE SECTION.
C
C INPUT QUANTITIES INCLUDE THE CORE TUBE DIMENSIONS (INNER RAD-
C IUS, OUTER RADIUS, AND LENGTH), A MAXIMUM VALUE OF THE BUCK-
C LING LOAD IMPROVEMENT RATIO TO BE STUDIED, AND AN INTEGER
C NUMBER OF EQUALLY SPACED STIFFENER ARC HEIGHTS TO BE ANALYZED.
C
C THE PROGRAM BEGINS BY CALCULATING ALLOWED STIFFENER THICKNESS
C FOR A SERIES OF STIFFENER ARC HEIGHTS (IE, 30, 60, 90, AND 120
C DEGREES) USING A RECURSIVE APPLICATION OF A DESIGN EQUATION
C DERIVED FROM THE STABILITY OF AN INFINITELY LONG CURVED PANEL
C CLAMPED ALONG ONE EDGE AND FREE ALONG THE OTHER. THIS PRO-
C CEDURE REQUIRES CALCULATING THE DEPLOYED INERTIA OF THE
C CROSS-SECTION AND THE CORRESPONDING OPTIMUM VALUE OF THE FIN
C DEPLOYMENT ANGLE FOR INITIAL APPROXIMATIONS OF THE CROSS-SECT-
C IONAL GEOMETRY. SUBSEQUENT APPROXIMATIONS ARE THEN DERIVED
C FROM THE PREVIOUS VALUES.
C
C FINALLY, THE SET OF INERTIAS AND AREAS ARE NORMALIZED TO THE
C INERTIA AND AREA OF CORE TUBE SO THAT A DATA FILE CAN BE GEN-
C ERATED FOR A PLOT OF NORMALIZED WEIGHT INCREASE VS. NORMALIZED
C BUCKLING LOAD IMPROVEMENT.
C
C INPUT VARIABLES ARE AS FOLLOWS:
C
C      RI      = INNER RADIUS OF TUBE
C      RO      = OUTER RADIUS OF TUBE (INNER OF STIFFENER)
C      L       = LENGTH OF COLUMN
C      PMAX    = RATIO OF MAXIMUM DESIGN BUCKLING LOAD
C               TO THAT OF THE CORE TUBE
C      NARC    = NUMBER OF STIFFENER ARC HEIGHTS
C               TO BE ANALYZED
C
C OTHER INTERNAL VARIABLES ARE AS FOLLOWS:
C
C      PHI     = DEPLOYMENT ANGLE OF STIFFENERS
C      PSI     = ARC HEIGHT OF STIFFENERS
C      RP      = OUTER RADIUS OF STIFFENERS
C
C .....
C      REAL IX, ICORE, INORM, L
C      CHARACTER*1 TAB
C      DIMENSION T(10), PDESIGN(10), WDESIGN(10), P(5,5), W(5,5)
C      TAB=Z'09'
C      IOUT=1
C      IDAT=2
C      WRITE (*,1)
C      WRITE (*,2)
C      OPEN(IOUT,FILE='STIFF. STRUT DESIGN.OUT',STATUS='NEW')

```

```

      OPEN(IDAT,FILE='STIFF. STRUT DESIGN.PLT',STATUS='NEW')
1  FORMAT (5X,28HDATA WILL BE SENT TO PRINTER)
2  FORMAT (5X,58HPLOT DATA WILL BE ECHOED TO FILE "STIFF. STRUT DE
XSIGN.PLT")
5  CONTINUE

C
C      READ IN DATA AND ECHO TO OUTPUT FILE
C
10  FORMAT (5X,32HINPUT INNER RADIUS OF TUBE (IN):)
20  FORMAT (5X,32HINPUT OUTER RADIUS OF TUBE (IN):)
30  FORMAT (5X,28HINPUT LENGTH OF COLUMN (IN):)
40  FORMAT (5X,48HINPUT MAXIMUM STRUT-TO-CORE BUCKLING LOAD RATIO:)
50  FORMAT (5X,48HINPUT NUMBER OF ARC HEIGHTS TO BE STUDIED (<10):)
60  FORMAT (10X,65H*****
1*****
70  FORMAT (10X,1H*,63X,1H*)
80  FORMAT (10X,65H*      GENERAL DESIGN OF A LATERALLY STIFFENED SL
1ENDER COLUMN      *)
90  FORMAT (10X,1H*,63X,1H*)
100  FORMAT (10X,65H*****
1*****//)
110  FORMAT (9X,24HINNER RADIUS OF TUBE  = ,F9.4,5H (IN))
120  FORMAT (9X,24HOUTER RADIUS OF TUBE  = ,F9.4,5H (IN))
130  FORMAT (9X,24HLENGTH OF TUBE        = ,F9.4,5H (IN))
140  FORMAT (9X,24HMAX. BUCKLING RATIO    = ,F9.6)
150  FORMAT (9X,24HNUMBER OF ARC HEIGHTS = ,I4)
      WRITE (*,10)
      READ (*,*) RI
      WRITE (*,20)
      READ (*,*) RO
      WRITE (*,30)
      READ (*,*) L
      WRITE (*,40)
      READ (*,*) PMAX
      WRITE (*,50)
      READ (*,*) NARC
      WRITE (IOUT,60)
      WRITE (IOUT,70)
      WRITE (IOUT,80)
      WRITE (IOUT,90)
      WRITE (IOUT,100)
      WRITE (IOUT,110) RI
      WRITE (IOUT,120) RO
      WRITE (IOUT,130) L
      WRITE (IOUT,140) PMAX
      WRITE (IOUT,150) NARC
      PI=ACOS(-1.0)

C
C      DETERMINE THE INERTIA AND AREA OF THE CORE TUBE
C
      ICORE=PI*((RO**4)-(RI**4))/4.
      ACORE=PI*((RO**2)-(RI**2))
      PSIINC=PI/(3*(NARC-1))
      PDESIGN(1)=1.0
      WDESIGN(1)=1.0

C
C      DETERMINE SET OF ALLOWABLE THICKNESSES USING A RECURSIVE

```

```

C      APPROACH.  THE FIRST STEP DETERMINES THE ALLOWED THICKNESS
C      BASED ON A FIRST GUESS AT THE RADIUS OF THE STIFFENER AND THE
C      RADIUS OF GYRATION OF THE STRUT EQUAL TO THE OUTER RADIUS OF
C      THE CORE.  THE SECOND AND SUBSEQUENT STEPS REFINE THE ESTIMATE
C      OF THE ALLOWED THICKNESS USING VALUES FOR THE STIFFENER RADIUS
C      AND RADIUS OF GYRATION BASED ON RESULTS FROM THE PREVIOUS GUESS.
C      ITERATION IS HALTED WHEN THE THICKNESS CONVERGES TO .5 PERCENT
C      (.005).  AT EACH ITERATION STEP, SUBPROGRAM "INERTIA" IS CALLED
C      TO CALCULATE THE OPTIMUM DEPLOYMENT ANGLE FOR THE GIVEN DESIGN.
C
C      THE DESIGN EQUATION COMES FROM EQUATING THE EULER STRESS
C      OF THE COLUMN TO THE LOCAL BUCKLING STRESS OF AN INFINITELY
C      LONG CURVED STIFFENER, CLAMPED ALONG ONE EDGE AND FREE ALONG
C      THE OTHER.
C
C      DO 400 I=1,NARC
C      ICOUNT=0
C      PSI=PSIINC*(I-1)+(PI/3.)
C      RHO=RO
C      RFIN=RO
C      T(I)=0.0
200    CONTINUE
C
C      BEGIN ITERATION TO DETERMINE ALLOWED THICKNESS FOR THE
C      GIVEN ARC HEIGHT.
C
C      ICOUNT=ICOUNT+1
C      TM1=T(I)
C      T(I)=RFIN*(110.*((RHO/L)**2)+.000974*PSI-.000669)
C      RP=RO+T(I)
C      CALL INERTIA (RI,RO,RP,IX,PHI,PSI)
C
C      CALCULATE STRUT AREA AND NEW RADIUS OF GYRATION
C
C      ATUBE=PI*((RP**2)-(RO**2))*(PSI*3)/(PI*2)+ACORE
C      RHO=SQRT(IX/ATUBE)
C      RFIN=RO+T(I)/2
C
C      TEST FOR CONVERGENCE AND CHECK THE MAXIMUM ITERATION
C      COUNTER.
C
C      IF (ICOUNT.EQ.1) GO TO 200
C      TEST=(T(I)/TM1)-1.0
C      TEST=ABS(TEST)
C      IF (ICOUNT.GE.20) GO TO 250
C      IF (TEST.GT.0.005) GO TO 200
250    CONTINUE
C      J=I+1
C      PDESIGN(J)=IX/ICORE
C      WDESIGN(J)=ATUBE/ACORE
C      PHIDEG=PHI*180/PI
C      PSIDEG=PSI*180/PI
C
C      PRINTOUT INERTIA AND AREA
C
260    FORMAT (/12X,21HARC HEIGHT OF FIN = ,F8.3,10H (DEG))
270    FORMAT (/13X,20HTHICKNESS OF FIN = ,E12.5,5H (IN))

```

```

280      FORMAT (5X,28HOPTIMUM DEPLOYMENT ANGLE = ,F8.3,10H      (
XDEG))
290      FORMAT (27X,6HIX = ,E12.5,7H(IN**4))
300      FORMAT (25X,8HAREA = ,E12.5,7H(IN**2)/)
      WRITE (IOUT,260) PSIDEG
      WRITE (IOUT,270) T(I)
      WRITE (IOUT,280) PHIDEG
      WRITE (IOUT,290) IX
      WRITE (IOUT,300) ATUBE
400 CONTINUE
C
C      ENTER LOOP TO DETERMINE A SERIES OF STRUT DESIGNS
C      FOR PSI=0, 30, 60, 90, 120 DEGREES. THIS DATA CAN
C      BE USED TO PLOT FOR COMPARISON WITH THE DESIGN
C      CURVES ALREADY GENERATED. BASE THE MAXIMUM THICKNESS
C      ON AN APPROXIMATION TO A BUCKLING LOAD = (PMAX*PCORE)
C
      TINC=(PMAX-1.)*ICORE/(52.67*(RO**3))
      TFIN=TCINC
      PSIINC=PI/6.
      DO 500 I=1,5
      P(I,1)=1.0
      W(I,1)=1.0
500 CONTINUE
      DO 520 J=2,5
      RP=RO+TFIN
      P(1,J)=PI*((RP**4)-(RI**4))/(4*ICORE)
      W(1,J)=PI*((RP**2)-(RI**2))/ACORE
      DO 510 I=2,5
      PSI=PSIINC*(I-1)
      CALL INERTIA (RI,RO,RP,IX,PHI,PSI)
      P(I,J)=IX/ICORE
      ATUBE=PI*((RP**2)-(RO**2))*(PSI**3)/(PI**2)
      X
      +ACORE
      W(I,J)=ATUBE/ACORE
510      CONTINUE
      TFIN=TFIN+TINC
520 CONTINUE
C
C      WRITE NORMALIZED INERTIAS AND AREAS TO OUTPUT
C      DATA FILE.
C
      DO 530 I=1,5
      WRITE (IDAT,530) (W(K,I),TAB,P(K,I),TAB,K=1,5)
530      FORMAT (10(F12.6,A1))
540      FORMAT (F12.6,A1,F12.6)
550 CONTINUE
      N=NARC+1
      DO 560 I=1,N
      WRITE (IDAT,540) WDESIGN(I),TAB,PDESIGN(I)
560 CONTINUE
      STOP
      END
      SUBROUTINE INERTIA (RI,RO,RP,IX,PHI,PSI)
C.....
C
C      SUBROUTINE INERTIA CALCULATES THE DEPLOYMENT ANGLE, PHI

```

```

C      WHICH GIVES THE MAXIMUM INERTIA FOR THE GIVEN RADII      .
C      (RI,RO,RP). USING THIS VALUE OF PHI, IT CALCULATES THE  .
C      AREA MOMENT OF INERTIA OF THE SECTION                     .
C                                                                .
C      INPUT VARIABLES ARE AS FOLLOWS:                          .
C                                                                .
C          RI      = INNER RADIUS OF TUBE                       .
C          RO      = OUTER RADIUS OF TUBE                       .
C                   (INNER RADIUS OF STIFFENERS)                .
C          RP      = OUTER RADIUS OF STIFFENERS                 .
C          PSI     = ARC HEIGHT OF STIFFENERS                   .
C                                                                .
C      OUTPUT VARIABLES ARE AS FOLLOWS:                          .
C                                                                .
C          IX      = MAXIMUM MOMENT OF INERTIA FOR CROSS-SECTION .
C          PHI     = DEPLOYMENT ANGLE FOR MAXIMUM INERTIA       .
C                                                                .
C.....
      REAL IX
      PI=ACOS(-1.0)
      A1=(PSI/8.0)*(RP**2-RO**2)*((RP+RO)**2)
      A2=(RP**3-RO**3)*(RP+RO)/3.0
      A3=3.0*PSI*(RP**4-RO**4)/8.0+PI*(RO**4-RI**4)/4.0

C
C      CALCULATE OPTIMUM DEPLOYMENT ANGLE
C
      BETA=(PI/2.)-(PSI/2.)+2.*ATAN((RP-RO)/(2.*(RP+RO)))
      PHI=ATAN((A2*SIN(PSI/2.)*COS(BETA))/
X(A2*SIN(PSI/2.)*SIN(BETA)-A1))
      IF (PHI.LT.0.) THEN
      PHI=PHI+PI
      ENDIF

C
C      DETERMINE INERTIA OF CROSS SECTION
C
      THETA=PI/2.0+PHI+2.0*ATAN((RP-RO)/(2.0*(RP+RO)))
      IX=3.*A1*(1.0-COS(PHI))+6.*A2*SIN(PHI/2.)*SIN(PSI/2.)
X*COS((PHI+PSI-2.*THETA)/2.)+A3
      RETURN
      END

```

APPENDIX C

VIBRATION FREQUENCIES OF THE STIFFENED COLUMN

Local vibration of truss members is a concern in the design of large space structures because of the desire to avoid interaction between local vibration modes and global vibration modes as well as active attitude control systems. Therefore, it is necessary to determine the effect deployable stiffeners have on the vibration frequency of the column in order to thoroughly evaluate their usefulness for application to large space structures.

The linearized expressions for column cross-sectional area and inertia given in Eq. 3.3 and 3.4 can be used to derive an approximation for the fundamental vibration frequency of the column. From this, an expression can be derived for percent increase in vibration frequency as a function of increase in mass and buckling load. Thus the general stiffened column design curves given in Fig. 3.7 can be amended to include information on vibration frequency increase.

The vibration frequency of interest corresponds to the half-sine wave lateral vibration of a pin-pinned column. The formula for this frequency is given in Eq. C-1 (21).

$$\omega = 9.87 \sqrt{\frac{EI}{\mu A l^4}} = \left(\frac{9.87}{l^2} \sqrt{\frac{E}{\mu}} \right) \sqrt{\frac{I}{A}} \quad (\text{C.1})$$

where μ is defined as the mass density of the material.

For the purpose of determining percent increase in vibration frequency, it is sufficient to consider the leading parenthetical phrase in Eq. C.1 to be a constant. Thus the vibration frequency is simply proportional to the square-root of the ratio of moment of inertia to area. Inserting Eq. 3.3 and 3.4 into Eq. C.1 and accounting for the additional deployment

mechanism mass, the following equations arise to describe the unstiffened (initial) vibration frequency (ω_o) and the stiffened vibration frequency (ω).

$$\omega_o = c\sqrt{\frac{t_{cc}}{t_{cc}}} = c \quad (C.2)$$

$$\omega = c\sqrt{\frac{t_{cc} + 4t_s}{t_{cc}(1 + M_m) + t_s}} = c\sqrt{\frac{1 + 4t_s/t_{cc}}{1 + M_m + t_s/t_{cc}}} \quad (C.3)$$

where:

$$c = \frac{9.87r}{l^2} \sqrt{\frac{E}{2\mu}}$$

The percent increase in vibration frequency from that of the unstiffened column is then simply:

$$\begin{aligned} \Delta\omega &= \frac{\omega_o - \omega}{\omega} = \frac{c\sqrt{\frac{1 + 4t_s/t_{cc}}{1 + M_m + t_s/t_{cc}}} - c}{c} \\ &= \sqrt{\frac{1 + 4t_s/t_{cc}}{1 + M_m + t_s/t_{cc}}} - 1 \end{aligned} \quad (C.4)$$

Eq. C.4 can be expressed in terms of the percent increase in column buckling load by noticing $\Delta P_{cr} = 4t_s/t_{cc}$, as shown in Chapter 3. This resulting expression is given in Eq. C.5.

$$\Delta\omega = \sqrt{\frac{1 + \Delta P_{cr}}{1 + M_m + .25\Delta P_{cr}}} - 1 \quad (C.5)$$

Setting $\Delta\omega$ to any constant value in Eq. C.5 results in an equation which is linear in P_{cr} . Furthermore it is possible to superimpose these lines of constant $\Delta\omega$ over the general stiffened column design curves presented in Fig. 3.7. Fig. C.1 presents the resulting plot.

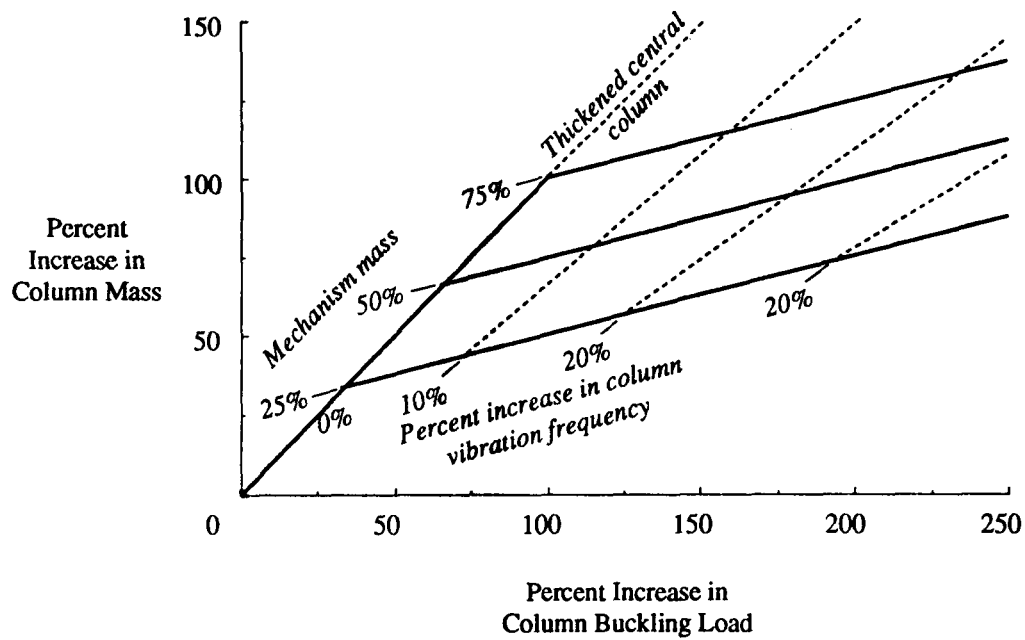


Figure C.1. General stiffened column design curves with vibration frequency increase.

Notice that the line corresponding to the thickened central column is also the line for which there is zero percent increase in vibration frequency. This result follows from Eq. C.2 in which it is shown that the vibration frequency of a thin walled circular column is independent of wall thickness. As expected, there is an increase in vibration frequency with the addition of deployable stiffeners just as there is an increase in column buckling load. However, it is important to note that the magnitude of increase in vibration frequency is typically much less than that for buckling load (e.g. approximately one order of magnitude less for a mechanism mass equal to 50%).

1. Report No. NASA TM-101636		2. Government Accession No.		3. Recipient's Catalog No.	
4. Title and Subtitle Stability and Dynamic Analysis of a Slender Column with Curved Longitudinal Stiffeners				5. Report Date August 1989	
				6. Performing Organization Code	
7. Author(s) Mark S. Lake				8. Performing Organization Report No.	
				10. Work Unit No. 506-43-31-02	
9. Performing Organization Name and Address NASA Langley Research Center Hampton, VA 23665-5225				11. Contract or Grant No.	
				13. Type of Report and Period Covered Technical Memorandum	
12. Sponsoring Agency Name and Address National Aeronautics and Space Administration Washington, DC 20546-0001				14. Sponsoring Agency Code	
15. Supplementary Notes					
16. Abstract This paper presents the results of a stability design study of a slender column with curved longitudinal stiffeners for large space structure applications. Linear stability analyses are performed using a "link-plate" representation of the stiffeners to determine stiffener local buckling stresses. Results from a set of parametric analyses are used to determine an approximate explicit expression for stiffener local buckling in terms of its geometric parameters. This expression along with other equations governing column stability and mass are assembled into a determinate system describing minimum mass stiffened column design. An iterative solution is determined to solve this system and a computer program incorporating this routine is presented. Example design problems are presented which verify the solution accuracy and illustrate the implementation of the solution routine. Also, observations are made which lead to a greatly simplified first iteration design equation relating the percent increase in column mass to the percent increase in column buckling load. From this, generalizations are drawn as to the mass savings offered by the stiffened column concept. Finally, the percent increase in fundamental column vibration frequency due to the addition of deployable stiffeners is studied.					
17. Key Words (Suggested by Author(s)) Stability Curved Stiffener Slender Column Mass			18. Distribution Statement Unclassified - Unlimited Subject Category - 39		
19. Security Classif. (of this report) Unclassified		20. Security Classif. (of this page) Unclassified		21. No. of pages 66	
				22. Price A04	